



Decays $h \rightarrow e_a e_b$, $e_b \rightarrow e_a \gamma$, and $(g - 2)_{e,\mu}$ in a 3-3-1 model with inverse seesaw neutrinos

T. T. Hong¹, N. H. T. Nha², T. Phong Nguyen², L. T. T. Phuong¹, and L. T. Hue^{1,3,4,*}

¹*An Giang University, VNU - HCM, Ung Van Khiem Street, Long Xuyen, An Giang 88000, Vietnam*

²*Department of Physics, Can Tho University, 3/2 Street, Ninh Kieu, Can Tho City 94000, Vietnam*

³*Subatomic Physics Research Group, Science and Technology Advanced Institute, Van Lang University, Ho Chi Minh City 70000, Vietnam*

⁴*Faculty of Applied Technology, School of Engineering and Technology, Van Lang University, Ho Chi Minh City 70000, Vietnam*

*E-mail: lethohue@vlu.edu.vn

Received June 20, 2022; Revised August 2, 2022; Accepted August 17, 2022; Published August 23, 2022

We will show that the 3-3-1 model with new heavy right-handed neutrinos as $SU(3)_L$ singlets can simultaneously explain the lepton flavor violating decays of the SM-like Higgs boson, charged lepton flavor violating decays $e_b \rightarrow e_a \gamma$, and the electron ($g - 2)_e$ anomalies under recent experimental data. The discrepancy of $(g - 2)_\mu$ predicted by the model under consideration and that of the standard model can reach 10^{-9} . The decay rates of the standard model-like Higgs boson $h \rightarrow \tau e, \tau \mu$ can reach values of $\mathcal{O}(10^{-4})$.

Subject Index B53, B54, B56, B59

1. Introduction

The experimental evidence of neutrino oscillation [1–5] confirms that the lepton flavor number is violated in the neutral lepton sector. This is great motivation to search for many lepton flavor violating (LFV) processes; the ones we focus on in this work are the LFV decays of the charged leptons $e_b \rightarrow e_a \gamma$ and the standard model-like (SM-like) Higgs boson (LFVH) $h \rightarrow e_a^\pm e_b^\mp$. The charged lepton flavor violating (cLFV) decays $e_b \rightarrow e_a \gamma$ are constrained by experiments as follows [6,7]:

$$\text{Br}(\tau \rightarrow \mu \gamma) < 4.4 \times 10^{-8}, \quad \text{Br}(\tau \rightarrow e \gamma) < 3.3 \times 10^{-8}, \quad \text{Br}(\mu \rightarrow e \gamma) < 4.2 \times 10^{-13}. \quad (1)$$

Upcoming sensitivities will be of order 10^{-9} and 10^{-14} for decays $\tau \rightarrow \mu \gamma, e \gamma$ [8,9] and $\mu \rightarrow e \gamma$ [10], respectively. LFVH decays have been investigated in many models beyond the standard model (BSM). On the other hand, the latest experimental constraints are: $\text{Br}(h \rightarrow \tau^\pm \mu^\mp) < 2.5 \times 10^{-3}$ [11], $\text{Br}(h \rightarrow \tau^\pm e^\mp) < 4.7 \times 10^{-3}$ [12], and $\text{Br}(h \rightarrow \mu^\pm e^\mp) < 6.1 \times 10^{-5}$ [13]. The future experimental sensitivities may be 1.4×10^{-4} , 1.6×10^{-4} , and 1.2×10^{-5} , respectively [14]. The small upper bounds of the cLFV branching rates suggest the explanation that they come from loop corrections relevant to LFV sources, including ones available in the neutral lepton sector. For models consisting of these necessary tree-level couplings to accommodate

neutrino oscillation data such as the Zee model [15], the constraints on the LFV sources such as Yukawa couplings are very strict [16,17]. Therefore, new scalar masses must not be heavier than 300 GeV in order to successfully explain the recent $(g - 2)$ data [16,18], while the LFVH decay rates are small [17,19].

To explain the neutrino oscillation data, the BSMs with the general seesaw (GSS) mechanism also result in LFV decays. But the versions adding only heavy seesaw type I neutrinos predict suppressed LFV rates that are much smaller than the upcoming experimental sensitivities [20,21]. In contrast, the models with only new inverse seesaw (ISS) neutrinos can predict large LFV rates. In addition, LFVH rates may be large in the regions satisfying constraints of $\text{Br}(e_b \rightarrow e_a \gamma)$ [22–25]. On the other hand, LFVH rates may be smaller when other constraints are considered [26,27]. In the supersymmetric (SUSY) versions of these models with new LFV sources from superparticles, LFVH rates may reach large orders of $\mathcal{O}(10^{-5})$ [20,28–36]. LFVH decays were also addressed with other experimental data in many other non-SUSY extensions of the SM [37–66]. Many BSMs predict that the strong constraints of cLFV decay rates $\text{Br}(e_b \rightarrow e_a \gamma)$ give small LFVH ones, or suppressed $(g - 2)_\mu$.

Unless there is some specific condition on the appearance of very light new bosons, the above cLFV constraints will result in small new one-loop contributions to the anomalous magnetic moments (AMMs) of charged leptons $(g - 2)_{e_a}/2 \equiv a_{e_a}$, in contrast with recent experimental data. Namely, the 4.2σ deviation between standard model (SM) prediction [68], combined contributions from previous works [69–94], and muon experiments [95,96] is

$$\Delta a_\mu^{\text{NP}} \equiv a_\mu^{\text{exp}} - a_\mu^{\text{SM}} = (2.51 \pm 0.59) \times 10^{-9}. \quad (2)$$

This result is slightly inconsistent with the latest one, which calculated the hadronic vacuum polarization for the SM prediction based on the lattice QCD approach, giving a combined value reported in Refs. [77,78,97] closer to the experimental data. This value was shown to fit with other experimental data such as global electroweak fits [98–100].

Regarding the electron anomaly, a 1.6σ discrepancy between SM and experiment was reported [101]:

$$\Delta a_e^{\text{NP}} \equiv a_e^{\text{exp}} - a_e^{\text{SM}} = (4.8 \pm 3.0) \times 10^{-13}. \quad (3)$$

The recent studies of cLFV decays in the regions satisfying the AMM data were done in some specific models such as SUSY with the largest $\text{Br}(h \rightarrow \tau \mu) \sim \mathcal{O}(10^{-4})$ [102]. Other BSMs containing leptoquarks can explain the large $\Delta a_\mu^{\text{NP}} \sim \mathcal{O}(10^{-9})$ [103].

Recent work has discussed an extension of the 3-3-1 model with right-handed neutrinos [104–106], named the 3-3-1 model with inverse seesaw neutrinos (331ISS) [107], with the aim of giving an explanation of both the $(g - 2)_\mu$ data and the neutrino oscillation data through the ISS mechanism. The model needs new $SU(3)_L$ gauge singlets including three neutral leptons X_{aR} and a new singly charged Higgs boson h^\pm to accommodate all the experimental data of neutrino oscillation, the cLFV bounds in Eq. (1), and the Δa_μ in 1σ deviation given in Eq. (2). Although cLFV and/or LFVH decays were investigated previously with promoting predictions for the 331ISS [108–111], the AMM data was not included. Our aim in this work is filling this gap. We note that other 3-3-1 models [112–115] constructed previously can accommodate the $(g - 2)_\mu$ data only when they are extended, such as adding new vector-like fermions or/and scalars [116–120]. But none of them paid attention to the correlations between LFVH decays and $(g - 2)_{e_a}$ anomalies.

Our paper is organized as follows. In Sect. 2 we discuss the necessary ingredients of a 331ISS model for studying LFVH decays and how the ISS mechanism works to generate active neutrino masses and mixing consistent with current experimental data. In Sect. 3 we present all the couplings needed to determine the one-loop contributions to the LFVH decay amplitudes of the SM-like Higgs boson, cLFV decays, and $(g - 2)_{e_a}$. In Sect. 4, we provide detailed numerical illustrations and discussions. Section 5 contains our conclusions. Finally, the appendix lists all of the analytic formulas expressing one-loop contributions to LFVH decay amplitudes calculated in the unitary gauge.

2. The 331ISS model for tree-level neutrino masses

2.1 Particle content and lepton masses

We summarize the particle content of the 331ISS model in this section. We ignore the quark sector irrelevant in our work, which was discussed previously [121,122]. We also ignore many detailed calculations presented in Ref. [107]. The electric charge operator defined by the gauge group $SU(3)_L \times U(1)_X$ is $Q = T_3 - \frac{1}{\sqrt{3}}T_8 + X$, where $T_{3,8}$ are diagonal $SU(3)_L$ generators. Each lepton family consists of an $SU(3)_L$ triplet $L_{aL} = (v_a, e_a, N_a)_L^T \sim (3, -\frac{1}{3})$ and a right-handed charged lepton $e_{aR} \sim (1, -1)$ with $a = 1, 2, 3$. The 331ISS model contains three neutral leptons $X_{aR} \sim (1, 0)$, $a = 1, 2, 3$, and a singly charged Higgs boson $\sigma^\pm \sim (1, \pm 1)$. There are three Higgs triplets $\rho = (\rho_1^+, \rho_0^0, \rho_2^+)^T \sim (3, \frac{2}{3})$, $\eta = (\eta_1^0, \eta^-_1, \eta_2^0)^T \sim (3, -\frac{1}{3})$, and $\chi = (\chi_1^0, \chi^-, \chi_2^0)^T \sim (3, -\frac{1}{3})$. The vacuum expectation values (VEVs) for generating all tree-level quark masses and leptons are $\langle \rho \rangle = (0, \frac{v_1}{\sqrt{2}}, 0)^T$, $\langle \eta \rangle = (\frac{v_2}{\sqrt{2}}, 0, 0)^T$, and $\langle \chi \rangle = (0, 0, \frac{w}{\sqrt{2}})^T$. Two neutral Higgs components have zero VEVs because of their non-zero generalized lepton numbers [107] corresponding to a new global symmetry $U(1)_L$ [122].

In the 331ISS model, nine gauge bosons get masses through the covariant kinetic Lagrangian of the Higgs triplets, $\mathcal{L}^H = \sum_{H=\chi, \eta, \rho} (D_\mu H)^\dagger (D^\mu H)$, where $D_\mu = \partial_\mu - ig \sum_{a=1}^8 W_\mu^a T^a - ig_X T^9 X X_\mu$, $a = 1, 2, \dots, 8$, and $T^9 \equiv \frac{I_3}{\sqrt{6}}$ and $\frac{1}{\sqrt{6}}$ for (anti)triplets and singlets [123]. There are two pairs of singly charged gauge bosons, denoted W^\pm and Y^\pm , defined as

$$W_\mu^\pm = \frac{W_\mu^1 \mp i W_\mu^2}{\sqrt{2}}, \quad Y_\mu^\pm = \frac{W_\mu^6 \pm i W_\mu^7}{\sqrt{2}}, \quad (4)$$

with the respective masses $m_W^2 = \frac{g^2}{4} (v_1^2 + v_2^2)$ and $m_Y^2 = \frac{g^2}{4} (w^2 + v_1^2)$. The breaking pattern of the model is $SU(3)_L \times U(1)_X \rightarrow SU(2)_L \times U(1)_Y \rightarrow U(1)_Q$, leading to the matching condition that W^\pm are the SM gauge bosons. As a consequence, we have

$$v_1^2 + v_2^2 \equiv v^2 = (246 \text{ GeV})^2, \quad \frac{g_X}{g} = \frac{3\sqrt{2}s_W}{\sqrt{3 - 4s_W^2}}, \quad gs_W = e, \quad (5)$$

where e and s_W are, respectively, the electric charge and sine of the Weinberg angle. Similarly to the two-Higgs doublet models (2HDM), we use the parameter

$$t_\beta \equiv \tan \beta = \frac{v_2}{v_1}, \quad (6)$$

which leads to $v_1 = vc_\beta$ and $v_2 = vs_\beta$.

The Yukawa Lagrangian generating lepton masses are:

$$\begin{aligned} \mathcal{L}_l^Y = & -h_{ab}^e \overline{L_a} \rho e_{bR} + h_{ab}^v \epsilon^{ijk} (\overline{L_a}_i (L_b)_j^c \rho_k^* - y_{ba}^X \overline{X_{bR}} \chi^\dagger L_a - \frac{1}{2} (\mu_X)_{ab} \overline{X_{aR}} (X_{bR})^c \\ & - Y_{ab}^\sigma \overline{(X_{aR})^c} e_{bR} \sigma^+ + \text{H.c.}, \end{aligned} \quad (7)$$

where $a, b = 1, 2, 3$. The first term generates charged lepton masses as $m_{e_a} \equiv \frac{h_{ab}^e v_1}{\sqrt{2}} \delta_{ab}$, with the assumption that the flavor states are also physical.

In the basis $n'_L = (v_L, N_L, (X_R)^c)^\top$, the Lagrangian in Eq. (7) generates a neutrino mass term written in terms of the total 9×9 mass matrix consisting of nine 3×3 sub-matrices [109], namely

$$-\mathcal{L}_{\text{mass}}^v = \frac{1}{2} \overline{(n'_L)^c} \mathcal{M}^v n'_L + \text{H.c.}, \quad \text{where } \mathcal{M}^v = \begin{pmatrix} \mathcal{O}_3 & m_D^\top & \mathcal{O}_3 \\ m_D & \mathcal{O}_3 & M_R^\top \\ \mathcal{O}_3 & M_R & \mu_X \end{pmatrix}, \quad (8)$$

where $(n'_L)^c = ((v_L)^c, (N_L)^c, X_R)^\top$, $(M_R)_{ab} \equiv y_{ab}^\chi \frac{w}{\sqrt{2}}$, and $(m_D^\top)_{ab} = -(m_D)_{ab} \equiv \sqrt{2} h_{ab}^v v_1$, with $a, b = 1, 2, 3$. The matrix μ_X in Eq. (7) is symmetric, and can be considered as a diagonal matrix without loss of generality.

The mass matrix \mathcal{M}^v is diagonalized by a 9×9 unitary matrix U^v ,

$$U^{v\top} \mathcal{M}^v U^v = \hat{M}^v = \text{diag}(m_{n_1}, m_{n_2}, \dots, m_{n_9}) = \text{diag}(\hat{m}_v, \hat{M}_N), \quad (9)$$

where m_{n_i} ($i = 1, 2, \dots, 9$) are masses corresponding to the physical states n_{iL} . The two mass matrices $\hat{m}_v = \text{diag}(m_{n_1}, m_{n_2}, m_{n_3})$ and $\hat{M}_N = \text{diag}(m_{n_4}, m_{n_5}, \dots, m_{n_9})$ consist of the masses of the active n_{aL} ($a = 1, 2, 3$) and extra neutrinos n_{IL} ($I = 1, 2, \dots, 6$), respectively. The following approximation solution of U^v is valid for any specific seesaw mechanisms,

$$U^v = \Omega \begin{pmatrix} U_{\text{PMNS}} & \mathcal{O}_{3 \times 6} \\ \mathcal{O}_{6 \times 3} & V \end{pmatrix}, \quad \Omega \simeq \begin{pmatrix} I_3 - \frac{1}{2} R R^\dagger & R \\ -R^\dagger & I_6 - \frac{1}{2} R^\dagger R \end{pmatrix}, \quad (10)$$

where R, V are 3×6 and 3×6 matrices, respectively. All entries of R must satisfy $|R_{aI}| \ll 1$, so that all ISS relations can be derived perturbatively.

The relations between the flavor and mass eigenstates are

$$n'_L = U^v n_L, \quad (n'_L)^c = U^{v*} (n_L)^c \equiv U^{v*} n_R, \quad (11)$$

where $n_L \equiv (n_{1L}, n_{2L}, \dots, n_{9L})^\top$, and the Majorana states are $n_i = (n_{iL}, n_{iR})^\top$.

The ISS relations are

$$R_2^* = m_D^\top M_R^{-1}, \quad R_1^* = -R_2^* \mu_X (M_R^\top)^{-1} \simeq \mathcal{O}_3, \quad (12)$$

$$m_v = R_2^* \mu_X R_2^\dagger = U_{\text{PMNS}}^* \hat{m}_v U_{\text{PMNS}}^\dagger = m_D^\top M_R^{-1} \mu_X (M_R^{-1})^\top m_D, \quad (13)$$

$$V^* \hat{M}_N V^\dagger = M_N + \frac{1}{2} M_N R^\dagger R + \frac{1}{2} R^\top R^* M_N. \quad (14)$$

From experimental data of m_v , we can determine all the independent parameters in m_D and three entries of $M^{-1} \equiv M_R^{-1} \mu_X (M_R^{-1})^\top$ [109,121]. Namely, the Dirac mass matrix has the antisymmetric form

$$m_D = z e^{i\alpha_{23}} \times \tilde{m}_D, \quad (15)$$

where $\alpha_{23} \equiv \arg[h_{32}^v]$, \tilde{m}_D is an antisymmetric matrix with $(\tilde{m}_D)_{23} = 1$, and

$$z = \sqrt{2} v_1 |h_{32}^v| = \sqrt{2} v_1 |h_{23}^v| = z_0 c_\beta \quad (16)$$

is a positive and real parameter. Equation (13) gives $(m_v)_{ij} = [m_D^\top M^{-1} m_D]_{ij}$ for all $i, j = 1, 2, 3$, leading to six independent equations. Solving three of them with $i \neq j$, the non-diagonal entries of M^{-1} are functions of M_{ii}^{-1} and $x_{12,13}$. Inserting these functions into the three remaining

relations with $i = j$, we obtain

$$(\tilde{m}_D)_{32} = \frac{(m_\nu)_{13}^2 - (m_\nu)_{11}(m_\nu)_{33}}{(m_\nu)_{13}(m_\nu)_{23} - (m_\nu)_{12}(m_\nu)_{33}}, \quad (\tilde{m}_D)_{21} = \frac{(m_\nu)_{12}(m_\nu)_{13} - (m_\nu)_{11}(m_\nu)_{23}}{(m_\nu)_{13}(m_\nu)_{23} - (m_\nu)_{12}(m_\nu)_{33}}, \quad (17)$$

and $\text{Det}[m_\nu] = 0$. From $M^{-1} = M_R^{-1}\mu_X(M_R^{-1})^\top$ we derive that three parameters of the matrix μ_X are certain but lengthy functions of $(ze^{i\alpha_{23}})$, all entries of M_R and m_ν . While m_ν are fixed by experiments, all entries of M_R are free parameters. We will fix $\alpha_{23} = 0$, because it is absorbed into μ_X .

In the limit $|R_2| \ll 1$, the heavy neutrino masses can be determined approximately based on Eq. (14), namely

$$V^* \hat{M}_N V^\dagger \simeq M_N. \quad (18)$$

We define the reduced matrix $M_R \equiv z\tilde{M}_R$, $(\tilde{M}_R)_{ij} \equiv k_{ij}$, provided that $R_2^* = -\tilde{m}_D/\tilde{M}_R$. The matrix M_R is always diagonalized by two unitary transformations $V_{L,R}$ [124]:

$$V_L^\top M_R V_R = z \times \hat{k} = z \times \text{diag}(\hat{k}_1, \hat{k}_2, \hat{k}_3), \quad (19)$$

where all $\hat{k}_{1,2,3}$ are always positive and $\hat{k}_a \gg 1$ so that all ISS relations are valid. Therefore, M_R is expressed in terms of \hat{k} and $V_{L,R}$. Then the matrix V in Eq. (14) can be found approximately as

$$V = \frac{1}{\sqrt{2}} \begin{pmatrix} V_R & iV_R \\ V_L & -iV_L \end{pmatrix} \rightarrow V^\top M_N V = z \times \begin{pmatrix} \hat{k} & \mathcal{O}_{3 \times 3} \\ \mathcal{O}_{3 \times 3} & \hat{k} \end{pmatrix}. \quad (20)$$

As a consequence, for any qualitative estimations we use the approximation that heavy neutrinos masses are $m_{n_{a+3}} = m_{n_{a+6}} \simeq z\hat{k}_a$ with $a = 1, 2, 3$; $R_1 \simeq \mathcal{O}_3$; and

$$U^\nu \simeq \begin{pmatrix} \left(I_3 - \frac{1}{2}R_2 R_2^\dagger\right) U_{\text{PMNS}} & \frac{1}{\sqrt{2}}R_2 V_L & \frac{-i}{\sqrt{2}}R_2 V_L \\ \mathcal{O}_3 & \frac{V_R}{\sqrt{2}} & \frac{iV_R}{\sqrt{2}} \\ -R_2^\dagger U_{\text{PMNS}} & \left(I_3 - \frac{R_2^\dagger R_2}{2}\right) \frac{V_R}{\sqrt{2}} & \left(I_3 - \frac{R_2^\dagger R_2}{2}\right) \frac{-iV_R}{\sqrt{2}} \end{pmatrix}. \quad (21)$$

We have checked and confirmed that the above approximations give numerical results consistent with those discussed in Ref. [107]. Therefore, these approximate formulas will be used in this work. m_ν is chosen as the input with 3σ neutrino oscillation data to fix \tilde{m}_D . The free parameters z_0 , $\hat{k}_{1,2,3}$, and V_R will be scanned in the valid ranges to construct the total neutrino mixing matrix U^ν defined in Eq. (21). Because

$$R_2 V_L = \tilde{m}_D^\dagger V_R^* \hat{k}^{-1}, \quad R_2 R_2^\dagger = \tilde{m}_D^\dagger V_R \hat{k}^{-2} \tilde{m}_D, \quad (22)$$

which do not depend explicitly on V_L , it has a weak effect on all relevant processes. We will fix $V_L = I_3$ from now on.

The Lagrangian for quark masses has been discussed previously [121, 122]. Here, we just recall that the Yukawa couplings of the top quark must satisfy the perturbative limit $h_{33}^u < \sqrt{4\pi}$, leading to a lower bound for v_2 : $v_2 > \frac{\sqrt{2}m_t}{\sqrt{4\pi}}$. Combined with the relations in Eqs. (5) and (6), the lower bound for t_β is $t_\beta \geq 0.3$. The upper bound for t_β can be derived from the tau mass, $m_\tau = h_{33}^3 \times vc_\beta \sqrt{2} \rightarrow h_{33}^3 = m_\tau \sqrt{2}/(vc_\beta) < \sqrt{4\pi}$, leading to the rather weak upper bound $t_\beta = \sqrt{1/c_\beta^2 - 1} \leq 346$.

2.2 Higgs bosons

The Higgs potential used here respects the new lepton number defined in Ref. [122], namely

$$\begin{aligned} V_h = & \sum_S \left[\mu_S^2 S^\dagger S + \lambda_S (S^\dagger S)^2 \right] + \lambda_{12}(\eta^\dagger \eta)(\rho^\dagger \rho) + \lambda_{13}(\eta^\dagger \eta)(\chi^\dagger \chi) + \lambda_{23}(\rho^\dagger \rho)(\chi^\dagger \chi) \\ & + \tilde{\lambda}_{12}(\eta^\dagger \rho)(\rho^\dagger \eta) + \tilde{\lambda}_{13}(\eta^\dagger \chi)(\chi^\dagger \eta) + \tilde{\lambda}_{23}(\rho^\dagger \chi)(\chi^\dagger \rho) + \sqrt{2}\omega f (\epsilon_{ijk} \eta^i \rho^j \chi^k + \text{h.c.}) \\ & + \sigma^+ \sigma^- \left[\mu_\sigma^2 + \sum_S \lambda_S^\sigma S^\dagger S \right] + [f_\eta(\rho^\dagger \eta)\sigma^+ + f_\chi(\rho^\dagger \chi)\sigma^+ + \text{h.c.}], \end{aligned} \quad (23)$$

where f is a dimensionless parameter, and $f_{\eta,\chi}$ are mass dimensional, $S = \eta, \rho, \chi$. These three trilinear couplings softly break the general lepton number \mathcal{L} . For simplicity, we fix $f_\chi = 0$ by applying a suitable discrete symmetry. The last line in Eq. (23) contains all additional terms coupling with new charged Higgs singlets compared with the Higgs potential considered in previous works [107]. They do not affect the squared mass matrices of both neutral CP-odd and CP-even Higgs bosons. The minimum conditions of the Higgs potential, as well as the identification of the SM-like Higgs boson, have previously been discussed in detailed [33,125], and hence we just list the necessary results here. The model contains three pairs of singly charged Higgs bosons $h_{1,2,3}^\pm$ and two Goldstone bosons $G_{W,Y}^\pm$ of the singly charged gauge bosons W^\pm and Y^\pm , respectively. In the limit of $f_\eta = 0$, the singly charged Higgs masses are $m_{h_1^\pm}^2 = \left(\frac{\tilde{\lambda}_{12} v^2}{2} + \frac{f w^2}{s_\beta c_\beta} \right)$, $m_{h_2^\pm}^2 = (v^2 c_\beta^2 + w^2) \left(\frac{\tilde{\lambda}_{23}}{2} + f t_\beta \right)$, and $m_{G_W^\pm}^2 = m_{G_Y^\pm}^2 = 0$ [125]. The mass of the Higgs singlet $\sigma \equiv h_3^\pm$ is a function of μ_σ^2 and λ_S^σ . With $f_\eta \neq 0$ as considered in this work, the relations between the original and mass eigenstates of the charged Higgs bosons are

$$\begin{pmatrix} \eta^\pm \\ \rho_1^\pm \\ \sigma^\pm \end{pmatrix} = \begin{pmatrix} -s_\beta & c_\alpha c_\beta & s_\alpha c_\beta \\ c_\beta & c_\alpha s_\beta & s_\alpha s_\beta \\ 0 & -s_\alpha & c_\alpha \end{pmatrix} \begin{pmatrix} G_W^\pm \\ h_1^\pm \\ h_2^\pm \end{pmatrix}, \quad \begin{pmatrix} \rho_2^\pm \\ \chi^\pm \end{pmatrix} = \begin{pmatrix} -s_\theta & c_\theta \\ c_\theta & s_\theta \end{pmatrix} \begin{pmatrix} G_Y^\pm \\ h_3^\pm \end{pmatrix}, \quad (24)$$

where $t_\theta = v_1/w$, and

$$\begin{aligned} f &= \frac{c_\beta s_\beta \left(2c_\alpha^2 m_{h_1^\pm}^2 + 2s_\alpha^2 m_{h_2^\pm}^2 - \tilde{\lambda}_{12} v^2 \right)}{2\omega^2}, \quad f_\eta = \frac{\sqrt{2}c_\alpha s_\alpha (m_{h_2^\pm}^2 - m_{h_1^\pm}^2)}{v}, \\ \mu_\sigma^2 &= \frac{1}{2} \left(2c_\alpha^2 m_{h_2^\pm}^2 - v^2 (c_\beta^2 \lambda_2^\sigma + s_\beta^2 \lambda_1^\sigma) + 2s_\alpha^2 m_{h_1^\pm}^2 - \lambda_3^\sigma \omega^2 \right). \end{aligned} \quad (25)$$

These results are consistent with Refs. [123,125,126] in the limits of $s_\alpha = 0, \pm 1$. The results given in Eqs. (24) and (25) were obtained by solving the following 3×3 squared mass matrix in the basis $(\eta^\pm, \rho_1^\pm, \sigma^\pm)$:

$$\mathcal{M}_c^2 = \begin{pmatrix} \frac{f\omega^2}{t_\beta} + \frac{1}{2}c_\beta^2 \tilde{\lambda}_{12} v^2 & f\omega^2 + \frac{1}{2}c_\beta \tilde{\lambda}_{12} s_\beta v^2 & \frac{c_\beta f_\eta v}{\sqrt{2}} \\ f\omega^2 + \frac{1}{2}c_\beta \tilde{\lambda}_{12} s_\beta v^2 & ft_\beta \omega^2 + \frac{1}{2}\tilde{\lambda}_{12} s_\beta^2 v^2 & \frac{f_\eta s_\beta v}{\sqrt{2}} \\ \frac{c_\beta f_\eta v}{\sqrt{2}} & \frac{f_\eta s_\beta v}{\sqrt{2}} & \frac{v^2}{2} \left(c_\beta^2 \lambda_2^\sigma + s_\beta^2 \lambda_1^\sigma \right) + \frac{\lambda_3^\sigma \omega^2}{2} + \mu_\sigma^2 \end{pmatrix}. \quad (26)$$

We will find out that the Higgs masses $m_{h_{1,2}^\pm}$ and the mixing angle α are functions of the Higgs parameters in the Higgs potential.

The model contains five CP-odd neutral scalar components included in the five neutral Higgs bosons $\eta_1^0 = (v_2 + R_1 + iI_1)/\sqrt{2}$, $\rho^0 = (v_1 + R_2 + iI_2)/\sqrt{2}$, $\chi_2^0 = (\omega + R_3 + iI_3)/\sqrt{2}$, $\eta_2^0 = (R_4 + iI_4)/\sqrt{2}$, and $\chi_1^0 = (R_5 + iI_5)/\sqrt{2}$. Three of them are Goldstones bosons of the neu-

tral gauge bosons Z , Z' , and X^0 . The two remaining are physical states with masses

$$m_{a_1}^2 = (s_\beta^2 v^2 + \omega^2) \left(f t_\beta^{-1} + \frac{1}{2} \tilde{\lambda}_{13} \right), \quad m_{a_2}^2 = f \left(\frac{\omega^2}{c_\beta s_\beta} + c_\beta s_\beta v^2 \right). \quad (27)$$

As a consequence, the parameter f must satisfy $f > 0$.

Considering the CP-even scalars, there are 2×2 and 3×3 sub-matrices for the masses of these Higgs bosons in two bases (η_2^0, χ_1^0) and $(\eta_1^0, \rho_1^0, \chi_1^0)$, namely

$$\begin{aligned} M_{0,3}^2 &= \begin{pmatrix} \frac{c_\beta f \omega^2}{s_\beta} + 2s_\beta^2 \lambda_1 v^2 & c_\beta s_\beta \lambda_{12} v^2 - \omega^2 f & \omega(s_\beta \lambda_{13} - c_\beta f)v \\ c_\beta s_\beta \lambda_{12} v^2 - \omega^2 f & \frac{s_\beta f \omega^2}{c_\beta} + 2c_\beta^2 \lambda_2 v^2 & \omega(c_\beta \lambda_{23} - s_\beta f)v \\ \omega(s_\beta \lambda_{13} - c_\beta f)v & \omega(c_\beta \lambda_{23} - s_\beta f)v & 2\lambda_3 \omega^2 + c_\beta s_\beta f v^2 \end{pmatrix}, \\ M_{0,2}^2 &= \begin{pmatrix} \frac{1}{2}\omega^2 \left(\tilde{\lambda}_{13} + \frac{2c_\beta f}{s_\beta} \right) & \frac{1}{2}\omega(\tilde{\lambda}_{13}s_\beta + 2c_\beta f)v \\ \frac{1}{2}\omega(\tilde{\lambda}_{13}s_\beta + 2c_\beta f)v & \frac{1}{2}s_\beta(\tilde{\lambda}_{13}s_\beta + 2c_\beta f)v^2 \end{pmatrix}. \end{aligned} \quad (28)$$

The matrix $M_{0,2}^2$ has one zero value and $m_{h_4}^2 = \left(\frac{f}{t_\beta} + \frac{\tilde{\lambda}_{13}}{2} \right) (s_\beta^2 v^2 + \omega^2)$ corresponding to one Goldstone boson of X^0 and a heavy neutral Higgs boson h_4^0 with mass at the $SU(3)_L$ breaking scale. On the other hand, we see that $\text{Det}[M_{0,3}^2] \neq 0$ but $\text{Det}[M_{0,3}^2]_{v=0} = 0$, which implies that there is at least one Higgs boson mass at the electroweak scale that can be identified with the SM-like Higgs boson. In particular, it can be proved that

$$C_1^h M_{0,3}^2 C_1^{hT} \Big|_{v=0} = \text{diag}(0, 2\lambda_3 w^2, f w^2 / (s_\beta c_\beta)), \quad C_1^h = \begin{pmatrix} s_\beta & c_\beta & 0 \\ -c_\beta & s_\beta & 0 \\ 0 & 0 & 1 \end{pmatrix}, \quad (29)$$

and $C_1^h M_{0,3}^2 C_1^{hT} \equiv M_{0,3}^2$ satisfying:

$$\begin{aligned} (M_{0,3}^2)_{11} &= 2v^2 (c_\beta^4 \lambda_2 + c_\beta^2 \lambda_{12} s_\beta^2 + \lambda_1 s_\beta^4), \\ (M_{0,3}^2)_{22} &= 2c_\beta^2 s_\beta^2 v^2 (\lambda_1 - \lambda_{12} + \lambda_2) + \frac{f \omega^2}{c_\beta s_\beta}, \\ (M_{0,3}^2)_{33} &= f c_\beta s_\beta v^2 + 2\lambda_3 \omega^2, \\ (M_{0,3}^2)_{12} &= (M_{0,3}^2)_{21} = c_\beta s_\beta v^2 (s_\beta^2 (\lambda_{12} - 2\lambda_1) - c_\beta^2 (\lambda_{12} - 2\lambda_2)), \\ (M_{0,3}^2)_{13} &= (M_{0,3}^2)_{31} = v\omega (-2f c_\beta s_\beta + c_\beta^2 \lambda_{23} + \lambda_{13} s_\beta^2), \\ (M_{0,3}^2)_{32} &= (M_{0,3}^2)_{23} = v\omega (f c_\beta^2 - f s_\beta^2 + c_\beta s_\beta (\lambda_{23} - \lambda_{13})). \end{aligned} \quad (30)$$

Therefore, there is a unitary transformation C_2^h with $(C_2^h)_{ij} \sim \mathcal{O}(v/w)$ ($i \neq j$) such that $C_2^h M_{0,3}^2 C_2^{hT} = \text{diag}(m_{h_1^0}^2, m_{h_2^0}^2, m_{h_3^0}^2)$ and $m_{h_i^0}^2 \sim \mathcal{O}(v^2)$ [109,127,128]. Hence, h_1^0 is identified with the SM-like Higgs boson found at the LHC, namely $h_1^0 \equiv h$. For simplicity we fix $C_2^h = I_3$ in this work, and use the relations $(\eta_1^0, \rho_1^0, \chi_1^0) = C_1^{hT}(h_1^0, h_2^0, h_3^0)$ in our numerical investigation, where only $\eta_1^0 \sim R_1$ and $\rho_1^0 \sim R_2$ give contributions to h_1^0 , namely

$$R_1 = s_\beta h_1^0 - c_\beta h_2^0, \quad R_2 = c_\beta h_1^0 + s_\beta h_2^0. \quad (31)$$

This assumption leads to the consequence that $m_{h_1^0}$ is independent of the Higgs self-couplings related to one-loop decays $h_1^0 \rightarrow e_a e_b$, as can be seen as follows:

$$-\mathcal{L}_h = V_h = \sum_{i,j=1}^3 -g_{hij} h_1^0 h_i^+ h_j^- + \dots, \quad (32)$$

where the non-zero $g_{h_1^0 ij} = g_{hji}$ are

$$\begin{aligned}
g_{h11} &= -vc_\alpha^2 \left[(2c_\beta^2 s_\beta^2 (\lambda_1 - \lambda_{12} + \lambda_2) + \lambda_{12} + \tilde{\lambda}_{12}) + t_\alpha^2 (c_\beta^2 \lambda_2^\sigma + s_\beta^2 \lambda_1^\sigma) + \frac{2s_\alpha^2 (m_{h_1^\pm}^2 - m_{h_2^\pm}^2)}{v^2} \right], \\
g_{h22} &= -vc_\alpha^2 \left[t_\alpha^2 (2c_\beta^2 s_\beta^2 (\lambda_1 - \lambda_{12} + \lambda_2) + \lambda_{12} + \tilde{\lambda}_{12}) + (c_\beta^2 \lambda_2^\sigma + s_\beta^2 \lambda_1^\sigma) - \frac{2s_\alpha^2 (m_{h_1^\pm}^2 - m_{h_2^\pm}^2)}{v^2} \right], \\
g_{h12} &= -c_\alpha s_\alpha v \left[2s_\beta^2 c_\beta^2 (\lambda_1 - \lambda_{12} + \lambda_2) - s_\beta^2 \lambda_1^\sigma - c_\beta^2 \lambda_2^\sigma + \lambda_{12} + \tilde{\lambda}_{12} - \frac{(c_\alpha^2 - s_\alpha^2) (m_{h_1^\pm}^2 - m_{h_2^\pm}^2)}{v^2} \right], \\
g_{h33} &= -v [c_\beta^2 (2c_\theta^2 \lambda_2 + s_\theta^2 (\lambda_{23} + \tilde{\lambda}_{23})) + s_\beta^2 (c_\theta^2 \lambda_{12} + \lambda_{13} s_\theta^2) + c_\beta c_\theta^2 (2f s_\beta + c_\beta \tilde{\lambda}_{23})]. \tag{33}
\end{aligned}$$

In the next section we derive all of the remaining couplings giving one-loop contributions of the decays mentioned in this work.

3. Couplings and analytic formulas

3.1 Decays $e_b \rightarrow e_a \gamma$ and $(g-2)_{e_a}$

The couplings of charged gauge bosons giving one-loop contributions to LFV amplitudes are:

$$L_{V^\pm ff} = \frac{g}{\sqrt{2}} \sum_{a=1}^3 \sum_{i=1}^9 \bar{n}_i \gamma^\mu P_L e_a \left[U_{ai}^{v*} W_\mu^+ + U_{(a+3)i}^{v*} Y_\mu^+ \right] + \text{h.c.} \tag{34}$$

All the calculation steps to derive these couplings were presented in Ref. [109]. From now on, we always choose that $m_{e_b} > m_{e_a}$, equivalently $b > a = 1, 2, 3$, to define the decays $e_b \rightarrow e_a \gamma$. One-loop form factors from charged gauge bosons are [129]:

$$\begin{aligned}
c_{(ab)R}(W) &= \frac{eg^2}{32\pi^2 m_W^2} \sum_{i=1}^9 U_{ai}^v U_{bi}^{v*} \tilde{F}_V(x_{W,i}), \\
c_{(ab)R}(Y) &= \frac{eg^2}{32\pi^2 m_Y^2} \sum_{i=1}^9 U_{(a+3)i}^v U_{(b+3)i}^{v*} \tilde{F}_V(x_{Y,i}), \tag{35}
\end{aligned}$$

where $x_{v,i} = m_{n_i}^2/m_v^2$; $v = W, Y$;

$$\tilde{F}_V(x) = -\frac{10 - 43x + 78x^2 - 49x^3 + 4x^4 + 18x^3 \ln(x)}{24(x-1)^4}, \tag{36}$$

$e = \sqrt{4\pi\alpha_{\text{em}}}$ is the electromagnetic coupling constant; and $g = e/s_W$.

The Yukawa couplings of charged Higgs bosons with leptons are defined by

$$\mathcal{L}^{\ell nh^\pm} = -\frac{g}{\sqrt{2}m_W} \sum_{k=1}^3 \sum_{a=1}^3 \sum_{i=1}^9 h_k^+ \bar{n}_i \left(\lambda_{ai}^{L,k} P_L + \lambda_{ai}^{R,k} P_R \right) e_a + \text{h.c.}, \tag{37}$$

where

$$\begin{aligned}\lambda_{ai}^{R,1} &= m_{e_a} c_\alpha t_\beta U_{ai}^{\nu*} - \sum_{c=1}^3 \frac{v Y_{ca}^\sigma s_\alpha}{\sqrt{2}} U_{(c+6)i}^{\nu*}, \quad \lambda_{ai}^{L,1} = c_\alpha s_\beta z_0 e^{i\alpha_{23}} \sum_{c=1}^3 (\tilde{m}_D)_{ac} U_{(c+3)i}^{\nu}, \\ \lambda_{ai}^{R,2} &= m_{e_a} s_\alpha t_\beta U_{ai}^{\nu*} + \sum_{c=1}^3 \frac{v Y_{ca}^\sigma c_\alpha}{\sqrt{2}} U_{(c+6)i}^{\nu*}, \quad \lambda_{ai}^{L,2} = s_\alpha s_\beta z_0 e^{i\alpha_{23}} \sum_{c=1}^3 (\tilde{m}_D)_{ac} U_{(c+3)i}^{\nu}, \\ \lambda_{ai}^{R,3} &= \frac{m_{e_a} c_\theta U_{(a+3)i}^{\nu*}}{c_\beta}, \quad \lambda_{ai}^{L,3} = c_\theta z_0 \sum_{c=1}^3 \left[-e^{i\alpha_{23}} (\tilde{m}_D)_{ac} U_{ci}^{\nu} + t_\theta^2 (\tilde{M}_R^T)_{ac} U_{(c+6)i}^{\nu} \right].\end{aligned}\quad (38)$$

The interactions given in Eqs. (34) and (37) also give tree and loop contributions to the lepton flavor conserved decay $\mu^- \rightarrow e^- \bar{\nu}_e \nu_\mu$. Regarding the gauge couplings given in Eq. (34), the couplings of Y^\pm with active neutrinos are zeros because $U_{(c+3)1}^\nu = U_{(c+3)2}^\nu = 0$, the difference of the couplings of W with active neutrinos and charged leptons between the SM and the 331ISS model under consideration is $| \frac{1}{2} (R_2 R_2^+ U)_{ab} | \ll 1$. Regarding the Higgs boson contributions, only $\lambda_{ai}^{L,3}$ may give large contributions to the decay amplitude $\mu^- \rightarrow e^- \bar{\nu}_e \nu_\mu$, because the remaining couplings are always proportional to $g m_\mu t_\beta / m_W \ll 1$ or $U_{(c+3)2}^\nu U_{(c+3)1}^\nu = 0$. Assuming $t_\theta = 0$ for very large $SU(3)_L$ scale $w \gg v$, we have a crude approximation that $|\lambda_{ai}^{L,3}| \leq z_0$. The large values of $|\lambda^{L,3}|$ appear because $h_3^\pm \simeq \rho_2^\pm$, which has couplings with active neutrinos $\bar{e}_a (\nu_{bL})^c \rho_2^- \sim h_{ab}^\nu \sim (\tilde{m}_D)_{ab}$ derived from the second term in the Lagrangian in Eq. (7). Based on the well-known formulas of the partial decay width $\Gamma(\mu \rightarrow 3e)$ at tree level given in the Zee–Babu model [141], the coupling λ^L leads to a deviation of the decay width of the decay $\mu^- \rightarrow e^- \bar{\nu}_e \nu_\mu$ between the 331ISS model and the SM as follows:

$$\begin{aligned}|\delta \Gamma^{331\text{ISS}}(\mu^- \rightarrow e^- \bar{\nu}_e \nu_\mu)| &\equiv \left| \frac{\Gamma^{331\text{ISS}}(\mu^- \rightarrow e^- \bar{\nu}_e \nu_\mu)}{\Gamma^{\text{SM}}(\mu^- \rightarrow e^- \bar{\nu}_e \nu_\mu)} - 1 \right| \\ &\simeq \left[\frac{|\lambda_{ai}^{L,3}|^2}{4m_{h_3^\pm}^2} \right]^2 = \left[\frac{|z_0|^2}{4m_{h_3^\pm}^2} \right]^2 \leq 10^{-6}.\end{aligned}\quad (39)$$

The constraint is derived from the mean lifetime of the muon [132]. The derivation of the formula in Eq. (39) is summarized as follows. The total amplitude is $i\mathcal{M} = i\mathcal{M}_W + i\mathcal{M}_{h^\pm}$, where \mathcal{M}_W and \mathcal{M}_{h^\pm} are the contributions from the W and charged Higgs bosons, respectively. In the low-energy limit we have

$$\begin{aligned}\mathcal{M}_W &\simeq \mathcal{M}^{\text{SM}} \sim \frac{g^2}{2m_W^2} [\bar{u}_{\nu_\mu} \gamma^\mu P_L u_\mu] [\bar{u}_e \gamma_\mu P_L v_{\nu_e}], \\ \mathcal{M}_{h^\pm} &\sim \frac{g^2}{2m_W^2 m_{h^\pm}^2} \times [\bar{u}_{\nu_\mu} (\lambda^L P_L + \lambda^R P_R) u_\mu] [\bar{u}_e (\lambda^{L*} P_R + \lambda^{R*} P_L) v_{\nu_e}].\end{aligned}$$

Now it can be proved that $|\mathcal{M}|^2 = |\mathcal{M}_W|^2 + |\mathcal{M}_{h^\pm}|^2$ because $\mathcal{M}_W^* \mathcal{M}_{h^\pm}$ has an odd number of gamma matrices in the trace and $m_e, m_{\nu_\mu}, m_{\nu_e} \simeq 0$, leading to $\mathcal{M}_W^* \mathcal{M}_{h^\pm} = 0$.

In the numerical investigation, we choose $m_{h_3^\pm} \geq z_0 \times 10\sqrt{5}$ to accommodate the constraint in Eq. (39). Now we can assume the approximation that $\Gamma^{331\text{ISS}}(\mu^- \rightarrow e^- \bar{\nu}_e \nu_\mu) \simeq \Gamma^{\text{SM}}(\mu^- \rightarrow e^- \bar{\nu}_e \nu_\mu)$. This approximation for calculating the cLFV decay rates is consistent with many works published recently [139, 140].

The one-loop form factors are [129]

$$c_{(ab)R}(h_k^\pm) = \frac{eg^2}{32\pi^2 m_W^2 m_{e_b} m_{h_k^\pm}^2} \sum_{i=1}^9 \left[\lambda_{ai}^{L,k*} \lambda_{bi}^{R,k} m_{n_i} F_H(x_{k,i}) + \left(m_{e_b} \lambda_{ai}^{L,k*} \lambda_{bi}^{L,k} + m_{e_a} \lambda_{ai}^{R,k*} \lambda_{bi}^{R,k} \right) \tilde{F}_H(x_{k,i}) \right], \quad (40)$$

where $b \geq a$, $x_{k,i} = m_{n_i}^2 / m_{h_k^\pm}^2$, and the one-loop functions $F_H(x)$ and $\tilde{F}_H(x)$ are

$$F_H(x) = -\frac{1-x^2+2x\ln(x)}{4(x-1)^3}, \quad \tilde{F}_H(x) = -\frac{-1+6x-3x^2-2x^3+6x^2\ln(x)}{24(x-1)^4}. \quad (41)$$

The total one-loop contributions to the cLFV amplitude $e_b \rightarrow e_a \gamma$ and $\Delta a_{e_a}^{331\text{ISS}}$ are

$$\begin{aligned} c_{(ab)R} &= \sum_{x=W,Y} c_{(ab)R}(x) + \sum_{k=1}^3 c_{(ab)R}(h_{1,2,3}^\pm), \\ c_{(ba)R} &= (c_{(ab)R}[a \leftrightarrow b]) \times \frac{m_{e_a}}{m_{e_b}}. \end{aligned} \quad (42)$$

The second line of Eq. (42) is derived from the equality $c_{(ba)R}(x) = (c_{(ab)R}(x)[b \leftrightarrow a]) \times (m_{e_a}/m_{e_b})$ for all $x = W, Y, h_{1,2,3}^\pm$. The formulas for the contributions to a_{e_a} are:

$$a_{e_a} = -\frac{4m_{e_a}^2}{e} \text{Re}[c_{(aa)R}] = -\frac{4m_{e_a}^2}{2\pi^2 v^2} \text{Re}[c'_{(aa)R}], \quad c'_{(ab)R} = c_{(ab)R} \times \left(\frac{eg^2}{32\pi^2 m_W^2} \right)^{-1}. \quad (43)$$

One-loop contributions from heavy neutral Higgs bosons are very suppressed, hence they are ignored here. The deviation of a_{e_a} between predictions by the two models 331ISS and SM is

$$\Delta a_{e_a} = \Delta a_{e_a}^{331\text{ISS}} \equiv a_{e_a} - a_{e_a}^{\text{SM}}(W), \quad (44)$$

where $a_\mu^{\text{SM}}(W) = 5g^2 m_\mu^2 / (96\pi^2 m_W^2)$ is the SM's prediction [130]. In this work, Δa_{e_a} is considered as new physics (NP) predicted by the 331ISS, used to compare with experimental data in numerical investigations.

The branching ratios of the cLFV processes are [129]

$$\text{Br}(e_b \rightarrow e_a \gamma) \simeq \frac{6\alpha_{em}}{\pi} \left(|c'_{(ab)R}|^2 + |c'_{(ba)R}|^2 \right) \text{Br}(e_b \rightarrow e_a \bar{v}_a v_b), \quad (45)$$

where $G_F = 1/(\sqrt{2}v^2)$, consistent with previous results [109,126] for 3-3-1 models.

The formulas for U^ν given in Eq. (21) result in approximate expressions for $c_{(ab)R}$ and $c_{(ba)R}$ with $b \geq a$ as follows:

$$\begin{aligned}
c'_{(ab)R}(W) &= -\frac{5}{12} \left[\delta_{ab} - (\tilde{m}_D^\dagger V_R \hat{k}^{-2} \tilde{m}_D)_{ab} \right] + \sum_{e=1}^3 (\tilde{m}_D^\dagger V_R^* \hat{k}^{-1})_{ae} (\tilde{m}_D^\dagger V_R \hat{k}^{-1})_{be} F_V(x'_{W,e}), \\
c'_{(ab)R}(Y) &= \frac{m_W^2}{m_Y^2} \sum_{e=1}^3 (V_R)_{ae}^* V_R)_{be} F_V(x'_{Y,e}), \\
c'_{(ab)R}(h_1^\pm) &= \frac{z_0^2}{m_{h_1^\pm}^2} \sum_{e=1}^3 (\tilde{m}_D^* V_R^*)_{ae} \left\{ c_\alpha^2 s_\beta^2 (\tilde{m}_D^\dagger V_R \hat{k}^{-1})_{be} - \frac{v s_{2\alpha} s_{2\beta}}{4m_b} [Y^{\sigma T} V_R]_{be} \right\} \hat{k}_e F_H(x'_{e,1}) \\
&\quad + \frac{c_\alpha^2 s_\beta^2 z_0^2}{m_{h_1^\pm}^2} \sum_{e=1}^3 (\tilde{m}_D V_R)_{ae}^* (\tilde{m}_D V_R)_{be} \tilde{F}_H(x'_{e,1}) \\
&\quad + \frac{1}{24} \left\{ \frac{m_{e_a}^2 c_\alpha^2 t_\beta^2}{m_{h_1^\pm}^2} \delta_{ab} + \frac{m_{e_a} v s_\alpha c_\alpha t_\beta}{\sqrt{2} m_{h_1^\pm}} \left[\frac{m_{e_a}}{m_{e_b}} (R_2 Y^\sigma)_{ab} + (Y^{\sigma\dagger} R_2^\dagger)_{ab} \right] \right\} \\
&\quad + \sum_{e=1}^3 \tilde{F}_H(x'_{e,1}) c_\alpha^2 \left\{ \frac{m_{e_a}^2 t_\beta^2}{m_{h_1^\pm}^2} [(R_2 V_L)_{ae} (R_2 V_L)_{be}^*] + \frac{v^2 t_\alpha^2 m_{e_a}}{m_{e_b} m_{h_1^\pm}^2} [(Y^{\sigma T} V_R)_{ae} (Y^{\sigma T} V_R)_{be}^*] \right. \\
&\quad \left. - \frac{m_{e_a} v s_\alpha c_\alpha t_\beta}{m_{h_1^\pm}^2} \left[\frac{m_{e_a}}{m_{e_b}} (R_2 V_L)_{ae} (Y^{\sigma T} V_R)_{be}^* + (Y^{\sigma T} V_R)_{ae} (R_2 V_L)_{be}^* \right] \right\}, \\
c'_{(ab)R}(h_2^\pm) &= c'_{(ab)R}(h_1^\pm) \left[m_{h_1^\pm} \rightarrow m_{h_2^\pm}, c_\alpha \rightarrow s_\alpha, s_\alpha \rightarrow -c_\alpha \right], \\
c'_{(ab)R}(h_3^\pm) &= \frac{z_0^2}{m_{h_3^\pm}^2} \left\{ \sum_{e=1}^3 \left[(\tilde{m}_D^* \tilde{m}_D V_R \hat{k}^{-1})_{ae} (V_R^*)_{be} k_e F_H(x'_{e,3}) \right] - \frac{1}{24} (\tilde{m}_D^* \tilde{m}_D)_{ab} \right. \\
&\quad \left. + \sum_{e=1}^3 \left[(\tilde{m}_D \tilde{m}_D^* V_R \hat{k}^{-1})_{ae} (\tilde{m}_D^* \tilde{m}_D V_R \hat{k}^{-1})_{be} + \frac{m_{e_a}^2}{z_0^2 c_\beta^2} (V_R^*)_{be} (V_R)_{ae} \right] \tilde{F}_H(x'_{e,3}) \right\}, \tag{46}
\end{aligned}$$

where the equalities in Eq. (22) were used. In addition, we ignore the minor contributions proportional to $R_2^\dagger R_2$ and $R_2 R_2^\dagger$. Because only two terms relating to $R_2 Y^\sigma$ and $R_2^\dagger R_2$ depend on V_L , but give small one-loop contributions to Δa_{e_a} , we fix $V_L = I_3$ without loss of generality.

The expressions for $c_{(ab)R}$ and $c_{(ba)R}$ given in Eq. (46) give some interesting properties. First, all terms are proportional to $1/m_{h_k^\pm}^2$, hence large $|\Delta a_{e_a}|$ corresponding to large $|c_{(aa)R}|$ will prefer small $m_{h_k^\pm}^2$. In contrast, experimental constraints on cLFV decay rates require small $|c_{(ab)R}|$ and $|c_{(ba)R}|$, hence $m_{h_k^\pm}^2$ should be large. It is easy to get small $\text{Br}(e_b \rightarrow e_a \gamma)$ with enough large $m_{h_k^\pm}$, but difficult to get large $|\Delta a_{e_a}|$. Previous numerical investigation has shown another situation [107], where small $m_{h_k^\pm}^2$ are needed for large Δa_μ , and the destructive correlations between particular terms in $c_{(ab)R}$ and $c_{(ba)R}$ must appear to result in small $\text{Br}(e_b \rightarrow e_a \gamma)$. The structure of the mass Dirac matrix \tilde{m}_D strongly affects these destructive correlations. As we will see, the antisymmetric property of \tilde{m}_D and the neutrino oscillation data fix a certain form of \tilde{m}_D , namely the fixed values considered in this work are $(\tilde{m}_D)_{32} = -(\tilde{m}_D)_{23} = 1$, $-(\tilde{m}_D)_{12} = (\tilde{m}_D)_{21} \simeq 0.613$, $-(\tilde{m}_D)_{13} = (\tilde{m}_D)_{31} \simeq 0.357$, and $(\tilde{m}_D)_{11} = (\tilde{m}_D)_{22} = (\tilde{m}_D)_{33} = 0$. They do not support large absolute values of the diagonal entries relating to $c_{(aa)R}$. Therefore, for the simple case of V_R

Table 1. Feynman rules for one-loop contributions to $(g - 2)$ anomalies, $e_b \rightarrow e_a \gamma$, and $h_1^0 \rightarrow e_a e_b$ in the unitary gauge; p_0 and p_{\pm} are the incoming momenta of h_1^0 and h_3^{\pm} , respectively.

Vertex	Coupling
$h_1^0 \bar{e}_a e_a$	$-\frac{igm_{e_a}}{2m_W}$
$h_1^0 \bar{n}_i n_j$	$-\frac{ig}{2m_W} (\lambda_{ij}^0 P_L + \lambda_{ij}^{0*} P_R)$
$h_k^+ \bar{n}_j e_b, h_k^- \bar{e}_a n_i$	$\frac{-ig}{\sqrt{2m_W}} (\lambda_{bi}^{L,k} P_L + \lambda_{bi}^{R,k} P_R),$ $\frac{-ig}{\sqrt{2m_W}} (\lambda_{ai}^{L,k*} P_R + \lambda_{ai}^{R,k*} P_L)$
$W_\mu^+ \bar{n}_i e_b, W_\mu^- \bar{e}_a n_i$	$\frac{ig}{\sqrt{2}} U_{ai}^{v*} \gamma^\mu P_L, \frac{ig}{\sqrt{2}} U_{ai}^v \gamma^\mu P_L$
$Y_\mu^+ \bar{n}_i e_b, Y_\mu^- \bar{e}_a n_i$	$\frac{ig}{\sqrt{2}} U_{(a+3)i}^{v*} \gamma^\mu P_L, \frac{ig}{\sqrt{2}} U_{(a+3)i}^v \gamma^\mu P_L$
$h_3^+ h_1^0 Y_\mu^-, h_3^- Y_\mu^+ h_1^0$	$\frac{i}{2} g c_\beta c_\theta (p_+ - p_0)^\mu, -\frac{i}{2} g c_\beta c_\theta (p_- - p_0)^\mu$
$h_1^0 W_\mu^+ W_\nu^-$	$ig m_W g^{\mu\nu}$
$h_1^0 Y_\mu^+ Y_\nu^-$	$ig c_\beta s_\theta m_Y g^{\mu\nu}$

$= I_3$, degenerate values of heavy neutrino masses $\hat{k}_{11} = \hat{k}_{22} = \hat{k}_{33}$ and $Y^\sigma = \mathcal{O}_{3 \times 3}$ will give $c_{(ab)R} \sim \tilde{m}_D \tilde{m}_D^*$. As a result, the constraints on cLFV decays always exclude the regions of parameter space predicting large $(g - 2)_{e,\mu}$. This conclusion is completely consistent with the numerical results reported in Ref. [107]. In addition, the presence of σ^\pm and non-zero Yukawa coupling matrix Y^σ is necessary to explain the 1σ range of $(g - 2)_\mu$ obtained by experiment. Additionally, the formulas given in Eq. (46) explain explicitly that large Δa_μ also needs large z_0 . Also, large t_β and non-zero Y^σ support more strong destructive correlations to guarantee that $(e_b \rightarrow e_a)$ satisfies the current constraints.

Finally, we emphasize that the $(g - 2)_e$ data and LFVH decays have not previously been discussed for the 331ISS model. Our numerical investigation showed that large $(g - 2)_e$ requires nonzero values of s_α , which was not considered in Ref. [107]. In addition, large values of $Y_{22,33,23,32}^\sigma$ should be investigated carefully because they may result in too-large $\text{Br}(h \rightarrow \tau \mu)$, which may be excluded by the experimental constraints.

3.2 Decays $h_1^0 \rightarrow e_a e_b$

The Yukawa couplings $h_1^0 f f$, namely

$$\mathcal{L}_{h_1^0 f f}^Y = -\frac{g}{2m_W} h_1^0 \left[\frac{1}{2} \sum_{i,j=1}^9 \bar{n}_i (\lambda_{ij}^0 P_L + \lambda_{ij}^{0*} P_R) n_j + m_{e_a} \bar{e}_a e_a \right], \quad (47)$$

where

$$\lambda_{ij}^0 = \sum_{c=1}^3 \left(U_{ci}^v U_{cj}^{v*} m_{n_i} + U_{ci}^{v*} U_{cj}^v m_{n_j} \right), \quad (48)$$

are symmetric coefficients $\lambda_{ij}^0 = \lambda_{ji}^0$ corresponding to the Feynman rules given in Ref. [124]. All of the Feynman rules for couplings involved in LFV processes at one-loop level are listed in Table 1, where we used $s_\theta = g v_1 / (2m_Y)$. We focus on the limit of tiny $t_\theta \simeq s_\theta = 0$, and the suppressed deviation of the SM-like Higgs mixing mentioned previously [109,127]. Namely, they will be fixed to be zeros in the numerical calculations.

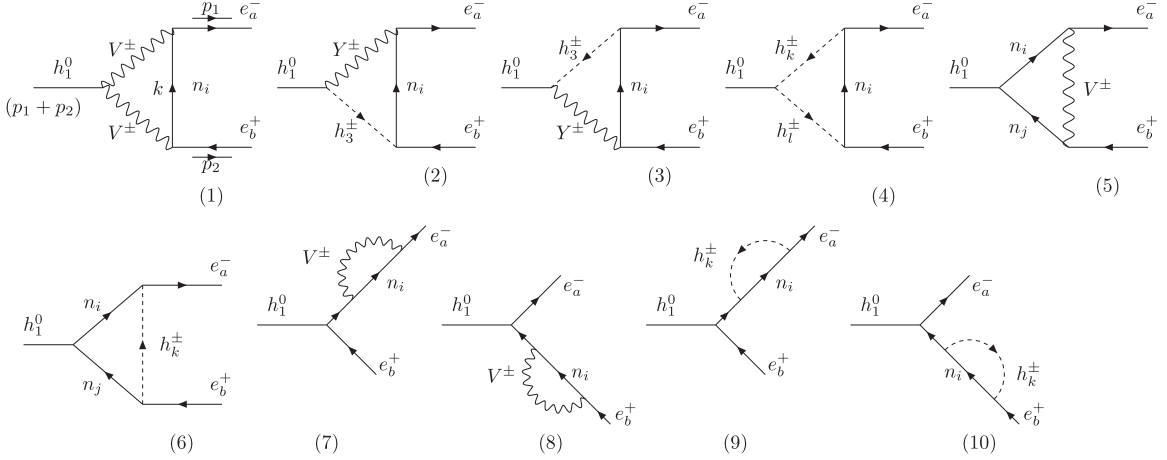


Fig. 1. One-loop Feynman diagrams contributing to the decay $h_1^0 \rightarrow e_a e_b$ in the unitary gauge. Here, $V^\pm = W^\pm, Y^\pm; k, l = 1, 2, 3$.

The effective Lagrangian and partial decay width of the decay $h_1^0 \rightarrow e_a^\pm e_b^\mp$ are

$$\mathcal{L}^{\text{LFVH}} = h_1^0 (\Delta_{(ab)L} \bar{e}_a P_L e_b + \Delta_{(ab)R} \bar{e}_a P_R e_b) + \text{H.c.},$$

$$\Gamma(h_1^0 \rightarrow e_a e_b) = \Gamma(h_1^0 \rightarrow e_a^- e_b^+) + \Gamma(h_1^0 \rightarrow e_a^+ e_b^-) = \frac{m_{h_1^0}}{8\pi} (|\Delta_{(ab)L}|^2 + |\Delta_{(ab)R}|^2), \quad (49)$$

where the scalar factors $\Delta_{(ab)L,R}$ are loop contributions here. In the unitary gauge, the one-loop Feynman diagrams contributing to $\Delta_{(ab)L,R}$ are shown in Fig. 1. The valid condition $m_{h_1^0} \gg m_{a,b}$ was used in Eq. (49), where $m_{a,b}$ are the lepton masses satisfying $p_{1,2}^2 = m_{a,b}^2$ and $p_{h_1^0}^2 \equiv (p_1 + p_2)^2 = m_{h_1^0}^2$. The branching ratio of LFVH decays is $\text{Br}(h_1^0 \rightarrow e_a e_b) = \Gamma(h_1^0 \rightarrow e_a e_b)/\Gamma_{h_1^0}^{\text{total}}$, where $\Gamma_{h_1^0}^{\text{total}} \simeq 4.1 \times 10^{-3} \text{ GeV}$ [131,132]. The $\Delta_{(ab)L,R}$ can be written as

$$\Delta_{(ab)L,R} = \sum_{i=1,5,7,8} \Delta_{(ab)L,R}^{(i)W} + \sum_{i=1}^{10} \Delta_{(ab)L,R}^{(i)Y}, \quad (50)$$

where the analytic forms of $\Delta_{(ab)L,R}^{(i)W}$ and $\Delta_{(ab)L,R}^{(i)Y}$ are shown in the appendix. There are a number of tiny one-loop contributions, which we will ignore in the numerical calculations. They are calculated using the unitary gauge with the same techniques given in Refs. [25,109]. The contributions from diagrams (2), (3), and (5) in Fig. 1 with Y^\pm exchanges have suppressed factors $c_\beta m_W^3/m_Y^3$. The one-loop contributions from diagram (6) are suppressed with heavy singly charged Higgs bosons, which we checked consistently with the result mentioned in Refs. [67,109].

4. Numerical discussion

In this work we use the neutrino oscillation data given in Refs. [132,133]. The standard form of the lepton mixing matrix U_{PMNS} is a function of three angles θ_{ij} , one Dirac phase δ , and two Majorana phases α_1 and α_2 [134], namely

$$U_{\text{PMNS}}^{\text{PDG}} = f(s_{12}, s_{13}, s_{23}, \delta) \times \text{diag}(1, e^{i\alpha_1}, e^{i\alpha_2}),$$

$$f(s_{12}, s_{13}, s_{23}, \delta) \equiv \begin{pmatrix} 1 & 0 & 0 \\ 0 & c_{23} & s_{23} \\ 0 & -s_{23} & c_{23} \end{pmatrix} \begin{pmatrix} c_{13} & 0 & s_{13}e^{-i\delta} \\ 0 & 1 & 0 \\ -s_{13}e^{i\delta} & 0 & c_{13} \end{pmatrix} \begin{pmatrix} c_{12} & s_{12} & 0 \\ -s_{12} & c_{12} & 0 \\ 0 & 0 & 1 \end{pmatrix}, \quad (51)$$

where $s_{ij} \equiv \sin \theta_{ij}$, $c_{ij} \equiv \cos \theta_{ij} = \sqrt{1 - s_{ij}^2}$, $i, j = 1, 2, 3$ ($i < j$), $0 \leq \theta_{ij} < 90^\circ$ and $0 < \delta \leq 360^\circ$. The Majorana phases are chosen in the range $-180^\circ \leq \alpha_i \leq 180^\circ$. For numerical investigation, we choose a benchmark corresponding to the normal order of the neutrino oscillation data as the input to fix \tilde{m}_D such that $s_{12}^2 = 0.32$, $s_{23}^2 = 0.547$, $s_{13}^2 = 0.0216$, $\Delta m_{21}^2 = 7.55 \times 10^{-5} [\text{eV}^2]$, $\Delta m_{32}^2 = 2.424 \times 10^{-3} [\text{eV}^2]$, $\delta = 180^\circ$, and $\alpha_1 = \alpha_2 = 0$. Consequently, the reduced Dirac mass matrix \tilde{m}_D is fixed as

$$\tilde{m}_D = \begin{pmatrix} 0 & 0.613 & 0.357 \\ -0.613 & 0 & 1 \\ -0.357 & -1 & 0 \end{pmatrix}. \quad (52)$$

The best-fit point for the normal (inverted) order is $\delta = -1.89^{+0.7}_{-0.58} (-1.38^{+0.48}_{-0.54}) \neq 180^\circ$ [133], which rules out the value 180° at 95% confidence level. But it is still allowed in the 3σ range. The other quantities corresponding to the best-fit point are $s_{23}^2 = 0.53$, $\Delta m_{21}^2 = 7.53 \times 10^{-5} [\text{eV}^2]$, $\Delta m_{32}^2 = 2.45 \times 10^{-3} [\text{eV}^2]$, leading to a new \tilde{m}_D with $(\tilde{m}_D)_{12} = 0.546 e^{0.18i}$ and $(\tilde{m}_D)_{13} = 0.453 e^{-0.23i}$. The existence of the non-zero CP violation $\delta \neq 180^\circ$ will lead to the complex values of the two entries of \tilde{m}_D instead of the real ones given in Eq. (52). These imaginary parts result in non-zero values of $\text{Im}[c_{(ab)R}]$, which is enough to give large $\text{Br}(\mu \rightarrow e\gamma) > 4.2 \times 10^{-13}$ in many regions of the parameter space, even when $\text{Re}[c_{(ab)R}] = 0$. Therefore, many very complicated relations between parameters must be satisfied to guarantee that all Im and Re parts contributing to these cLFV decays satisfy the experimental constraints. In this work, the limit $\delta = 180^\circ$ is fixed for simplicity.

The mixing matrix V_R is parameterized using the formulas given in Eq. (51), $V_R = f(s_{12}^r, s_{13}^r, s_{23}^r, 0)$ with $|s_{ij}^r| \leq 1$. The remaining free parameters are scanned in the following ranges:

$$\begin{aligned} \hat{k}_{1,2,3} &\geq 5, \quad 600 [\text{GeV}] \leq m_{h_{1,2}^\pm} \leq 1500 [\text{GeV}], \quad |s_\alpha| \leq 1, \quad \max[|Y_{ij}^\sigma|] \leq 1.5, \\ t_\beta &\in [30, 70], \quad 400 [\text{GeV}] \leq z \leq 1200 [\text{GeV}], \end{aligned} \quad (53)$$

and $m_{h_3^\pm} = 40 \text{ TeV}$, so that the decay width of $\mu^- \rightarrow e^- \bar{\nu}_e \nu_\mu$ is consistent with that predicted by the SM. In addition, the collected points satisfy $\max|(R_2 R_2^\dagger)_{ab}| < 10^{-3}$ with all $a, b = 1, 2, 3$. This constraint also satisfies many other recent experimental results such as electroweak precision tests and cLFV decays [142–145]. The experimental parameters are $G_F = 1.663787 \times 10^{-5} [\text{GeV}^{-2}]$, $g = 0.652$, $\alpha_{em} = e^2/(4\pi) = 1/137$, $s_W^2 = 0.231$, $m_e = 5 \times 10^{-4} [\text{GeV}]$, $m_\mu = 0.105 [\text{GeV}]$, $m_\tau = 1.776 [\text{GeV}]$, $m_W = 80.385 [\text{GeV}]$, $\text{Br}(\mu \rightarrow e \bar{\nu}_e \nu_\mu) \simeq 1$, $\text{Br}(\tau \rightarrow e \bar{\nu}_e \nu_\tau) \simeq 0.1782$, and $\text{Br}(\tau \rightarrow \mu \bar{\nu}_\mu \nu_\tau) \simeq 0.1739$. We note that the upper bounds of $m_{h_{1,2}^\pm}$ and t_β are based on the previous work to accommodate large values of Δa_μ . Chosen the scanning range of t_β also satisfies the perturbative limit mentioned above.

We comment here on the results obtained previously in Ref. [107], where large $t_\beta \geq 50$ and small values of singly charged Higgs bosons h_k^\pm ($k = 1, 2$) are required for large $(g - 2)_\mu$ satisfying the 1σ experimental data of $(g - 2)_\mu$ and all constraints from cLFV decays $e_b \rightarrow e_a \gamma$. But only the case of $s_\alpha = 0$ and non-zero $Y_{22,33,23,32}^\sigma$ was mentioned. Our numerical investigation shows that this case results in small Δa_e , which cannot satisfy the 1σ range of the experimental data given in Eq. (3). Without σ^\pm , we obtain two maximal values of Δa_e that $\Delta a_e \leq 2.5 \times 10^{-14}$ and 1.5×10^{-14} for the NO and IO schemes, respectively. Hence, determining the regions of parameter space giving large Δa_e will be very interesting.

For the above reasons, we focus on the regions of parameter space giving a large Δa_e that satisfies the 1σ experimental data of $(g - 2)_e$ as well as all current constraints of cLFV decay rates $\text{Br}(e_b \rightarrow e_a \gamma)$. The investigation shows that the 1σ range of $\Delta a_e \in [1.8 \times 10^{-13}, 7.8 \times 10^{-13}]$ can be obtained easily in a wide range of the parameter space, for example with the following fixed values of $z_0 = 500 \text{ GeV}$, $t_\beta = 50$, and $s_\alpha = 0.5$, and scanning the remaining parameters, we have a benchmark point that $m_{h_1^\pm} = 814.8 \text{ GeV}$, $m_{h_2^\pm} = 771.5 \text{ GeV}$, $m_{n_4} = m_{n_7} = 2.152 \text{ TeV}$, $m_{n_5} = m_{n_8} = 4.365 \text{ TeV}$, $m_{n_6} = m_{n_9} = 3.156 \text{ TeV}$, $s_{12}^r = -0.075$, $s_{13}^r = -0.565$, $s_{23}^r = -0.063$, and $0 \leq |Y_{ab}^\sigma| \leq 0.293$, which results in the following allowed values of the relevant physical processes: $\Delta a_e = 4.243 \times 10^{-13}$, $\Delta a_\mu = 1.019 \times 10^{-9}$, $\text{Br}(\mu \rightarrow e\gamma) = 2.95 \times 10^{-13}$, $\text{Br}(\tau \rightarrow e\gamma) = 6.18 \times 10^{-9}$, $\text{Br}(\tau \rightarrow \mu\gamma) = 3.52 \times 10^{-8}$, $\text{Br}(h_1^0 \rightarrow \mu e) = 1.59 \times 10^{-7}$, $\text{Br}(h_1^0 \rightarrow \tau e) = 6.56 \times 10^{-6}$, and $\text{Br}(h_1^0 \rightarrow \tau \mu) = 2.7 \times 10^{-4}$.

We list here other interesting benchmark points of the parameter space corresponding to large $t_\beta = 60$ that satisfy the 1σ range of $(g - 2)_e$, $\Delta a_\mu \geq 0.6 \times 10^{-9}$, and all current LFV upper bounds. For other large t_β values, the results are the same.

- (1) A benchmark point giving large $\text{Br}(h_1^0 \rightarrow \tau e) \sim \mathcal{O}(10^{-5})$:

$$\begin{aligned} \{z_0[\text{GeV}], t_\beta, s_\alpha\} &= \{867.7, 60, 0.460\}, \{s_{12,13,23}^r\} = \{0.377, 0.556, -0.907\}, \\ \{m_{h_{1,2}^\pm}[\text{TeV}]\} &= \{0.974, 0.918\}, \{m_{4,5,6} = m_{7,8,9}[\text{TeV}]\} = \{3.32, 5.265, 3.341\}, \\ Y^\sigma &= \begin{pmatrix} 0.015 & 0.006 & -0.013 \\ -0.044 & 0.047 & -0.108 \\ 0.003 & -0.183 & 0.063 \end{pmatrix}. \end{aligned}$$

The corresponding values of $\Delta a_{e,\mu}$ and LFV decay rates are

$$\begin{aligned} \Delta a_e &= 5.89 \times 10^{-13}, \Delta a_\mu = 1.077 \times 10^{-9}, \\ \text{Br}\{(\mu \rightarrow e\gamma), (\tau \rightarrow e\gamma), (\tau \rightarrow \mu\gamma)\} &= \{8.31 \times 10^{-14}, 1.28 \times 10^{-8}, 4.04 \times 10^{-8}\} \\ \text{Br}(h_1^0 \rightarrow \{\mu e, \tau e, \tau \mu\}) &= \{5.9 \times 10^{-7}, 5.91 \times 10^{-5}, 5.18 \times 10^{-4}\}. \end{aligned}$$

- (2) There exists a benchmark point that allows large $\text{Br}(h_1^0 \rightarrow \tau e) \sim \mathcal{O}(10^{-5})$, but small $\text{Br}(h_1^0 \rightarrow \tau \mu) < \mathcal{O}(10^{-7})$:

$$\begin{aligned} \{z_0[\text{GeV}], t_\beta, s_\alpha\} &= \{478.5, 60, 0.993\}, \{s_{12,13,23}^r\} = \{0.629, -0.867, -0.818\}, \\ \{m_{h_{1,2}^\pm}[\text{TeV}]\} &= \{0.997, 0.864\}, \{m_{4,5,6} = m_{7,8,9}[\text{TeV}]\} = \{2.994, 4.092, 2.378\}, \\ Y^\sigma &= \begin{pmatrix} 0.069 & 0.164 & -0.085 \\ -0.076 & 0.058 & -0.199 \\ 0.074 & -0.180 & -0.086 \end{pmatrix}, \end{aligned}$$

$$\begin{aligned} \Delta a_e &= 4.67 \times 10^{-13}, \Delta a_\mu = 0.998 \times 10^{-9}, \\ \text{Br}\{(\mu \rightarrow e\gamma), (\tau \rightarrow e\gamma), (\tau \rightarrow \mu\gamma)\} &= \{2.196 \times 10^{-13}, 3.523 \times 10^{-9}, 3.547 \times 10^{-8}\}, \\ \text{Br}(h_1^0 \rightarrow \{\mu e, \tau e, \tau \mu\}) &= \{5.93 \times 10^{-6}, 1.88 \times 10^{-5}, 6.56 \times 10^{-8}\}. \end{aligned}$$

- (3) There exists a benchmark point predicting large $\text{Br}(h \rightarrow e\mu) \sim \mathcal{O}(10^{-5})$, which is close to the experimental constraint:

$$\{z_0[\text{GeV}], t_\beta, s_\alpha\} = \{1019.5, 60, 0.848\}, \{s_{12,13,23}^r\} = \{0.11, -0.89, -0.822\},$$

$$\{m_{h_{1,2}^\pm}[\text{TeV}]\} = \{0.671, 0.622\}, \{m_{4,5,6} = m_{7,8,9}[\text{TeV}]\} = \{6.533, 9.657, 4.414\},$$

$$Y^\sigma = \begin{pmatrix} 0.079 & 0.189 & -0.113 \\ -0.094 & -0.061 & -0.210 \\ 0.079 & -0.241 & -0.059 \end{pmatrix},$$

$$\Delta a_e = 3.19 \times 10^{-13}, \Delta a_\mu = 0.917 \times 10^{-9},$$

$$\text{Br}\{\mu \rightarrow e\gamma, (\tau \rightarrow e\gamma), (\tau \rightarrow \mu\gamma)\} = \{2.37 \times 10^{-13}, 2.80 \times 10^{-9}, 3.07 \times 10^{-8}\},$$

$$\text{Br}(h_1^0 \rightarrow \{\mu e, \tau e, \tau \mu\}) = \{1.85 \times 10^{-5}, 1.05 \times 10^{-4}, 1.48 \times 10^{-3}\}.$$

It is noted that large $\text{Br}(h \rightarrow e\mu)$ requires both large z_0 and $\text{Br}(h \rightarrow \tau\mu) \sim \mathcal{O}(10^{-3})$, which may be excluded by planned experiments. In this case, the numerical results show that $\text{Br}(h \rightarrow \tau\mu) < \mathcal{O}(10^{-4})$ will lead to $\text{Br}(h \rightarrow e\mu) < \mathcal{O}(10^{-6})$, which is still smaller than the planned experimental sensitivity.

From our numerical investigation, we found that the regions allowing 1σ range of Δa_e data and cLFV constraints are very wide. But the regions allowed large $(g - 2)_\mu$ are difficult to control. This is because of the large number of free parameters in the 331ISS: our numerical code is still not smart enough to collect these points. Because of the special form of \tilde{m}_D , we require a non-degenerate matrix \hat{k} and strong destructive correlations between the mixing angles s_{ab}^r and the entries of Y^σ in order to get small $\text{Br}(e_b \rightarrow e_a\gamma)$ in the regions that allow large Δa_μ . There may exist some relations between these parameters for collecting more interesting points allowing large $(g - 2)_\mu$ at 1σ experimental range. We will determine them in a future work.

Finally, we comment on some properties of the current Z boson decay data which may put useful constraints on the parameter space of the 331ISS model. In the limit of $v/w \rightarrow 0$, equivalently $t_\theta = 0$, for the couplings of the Z boson with all other SM particles we can see that all masses of the new heavy neutrinos appearing in the collected points we showed above as the numerical results are much larger than the Z boson masses. Therefore, Z bosons do have not any new tree-level decays $Z \rightarrow \bar{n}_I n_j$ with at least a new heavy neutrino n_I ($I > 3$). In addition, all the masses of the new heavy particles predicted by the 331ISS models are heavier than the Z boson masses, and therefore the invisible decays of the Z boson in this case are the same as in the SM and the 2HDM discussed in Ref. [67]. We therefore conclude that the current Z boson decay data weakly affects the allowed region of the parameters space we focus on this work.

There is another cLFV decay mode $Z \rightarrow e_a^+ e_b^-$ discussed in detailed in 2HDM [67], which is still invisible in the regions predicting large $\text{Br}(h \rightarrow e_a e_b)$ and satisfying all the constraints of cLFV decays $\text{Br}(e_b \rightarrow e_a\gamma)$. Therefore, this decay channel will not change significantly the allowed regions of parameters discussed in this work. On the other hand, the interesting topic we will focus on is that when the experimental sensitivities are improved, both cLFV decays of

$\mu^- \rightarrow e^- \bar{\nu}_e \nu_\mu$ and $Z \rightarrow e_a e_b$ may give more significant constraints on those mentioned in this work.

5. Conclusion

In this work we have constructed analytic formulas for one-loop contributions to the LFV decays of the SM-like Higgs boson $h_1^0 \rightarrow e_a e_b$ in the 331ISS model. We also give analytic formulas to explain qualitatively the results of the large $(g - 2)_\mu$ previously reported. Numerical tests were used to confirm the consistency between the two calculations. We introduced a new parameterization of the heavy neutrino mass matrix to reduce the number of free parameters used to investigate $(g - 2)_{e,\mu}$ anomalies, LFV decays $e_b \rightarrow e_a \gamma$, and $h_1^0 \rightarrow e_a e_b$. Our numerical investigation shows that the model can predict easily the 1σ range of experimental data for $(g - 2)_e$ and simultaneously satisfy the cLFV constraints on $\text{Br}(e_b \rightarrow e_a \gamma)$. But we only obtained the regions of parameter space that give the largest values of $\Delta a_\mu \simeq 10^{-9}$, which is rather smaller than the lower bound of the 1σ range reported recently. The reason is that the recent numerical code used in our investigation only works in the limit of small $\max[|y^\sigma|] < 0.25$. In these regions of the parameter space, the largest values of $\text{Br}(h_1^0 \rightarrow \tau e)$ and $\text{Br}(h_1^0 \rightarrow \tau \mu)$ are order of $\mathcal{O}(10^{-4})$ and 10^{-3} , respectively. In addition, large $\text{Br}(h_1^0 \rightarrow \tau \mu)$ predicts large $\text{Br}(h_1^0 \rightarrow \mu e) \sim \mathcal{O}(10^{-5})$, which is close to the recent experimental bounds. The regions with large $|Y^\sigma|_{ab}$ may be more interesting, which is our future work, where many other LFV processes such as $Z \rightarrow e_b e_a$, $e_b \rightarrow e_c e_d e_f$, and the $\mu-e$ conversion in nuclei will be discussed together.

Acknowledgments

We are grateful to Prof. Martin Hofericher and Dr Mukesh Kumar for their communications. We would like to thank the referee for reminding us of the important contribution of the singly charged Higgs bosons to the decay $\mu^- \rightarrow e^- \bar{\nu}_e \nu_\mu$, which significantly changes our numerical results. This research is funded by An Giang University under grant number 21.01.TB. L. T. Hue is grateful to Van Lang University.

Funding

Open Access funding: SCOAP³.

Appendix A. Form factors of LFVH in the unitary gauge

The one-loop contributions here are calculated using the notations of Passarino–Veltman (PV) functions [135,136] given in Ref. [27], consistent with LoopTools [137]; see detailed discussions in Refs. [33,138]. The PV functions used in this work are defined as follows: $B_\mu^{(i)} \equiv B_1^{(i)} \times (-1)^i p_{i\mu}$ with $i = 1, 2$, and $C_\mu \equiv \sum_{i=1}^2 (-1)^i p_{i\mu} \times C_i$. As mentioned in Ref. [27], the two $B_1^{(1)}$ and C_1 have opposite signs to those introduced in Ref. [33]. They come from the signs of $p_{1,2}$ in the internal momenta $(k - p_1)$ and $(k + p_2)$ shown in Fig. 1, where p_1 has an opposite sign, which is different from the standard notation of $k + p_1$ defined in LoopTools. The PV functions used in our formulas are: $B_{0,1}^{(i)} = B_{0,1}(p_i^2; M_0^2, M_i^2)$, $C_{0,1,2} = C_{0,1,2}(p_1^2, (p_1 + p_2)^2, p_2^2; M_0^2, M_1^2, M_2^2)$, and $B_0^{(12)} = B_0((p_1 + p_2)^2; M_1^2, M_2^2)$. In the following, when the external momenta are fixed as $p_1^2 = m_{e_a}^2$, $p_2^2 = m_{e_b}^2$, and $(p_1 + p_2)^2 = m_{h_1^0}^2$, we use simpler notation as follows: $C_{0,1,2}(p_1^2, m_{h_1^0}^2, p_2^2; M_0^2, M_1^2, M_2^2) \equiv C_{0,1,2}(M_0^2, M_1^2, M_2^2)$, $B_{0,1}^{(i)}(M_0^2, M_i^2) = B_{0,1}(p_i^2; M_0^2, M_i^2)$, and $B_0(m_{h_1^0}^2; M_1^2, M_2^2) = B_0^{(12)}(M_1^2, M_2^2)$.

The analytic expressions $\Delta_{L,R}^{(i)W} \equiv \Delta_{(ab)L,R}^{(i)W}$ for one-loop contributions from diagram (1) in Fig. 1 are

$$\begin{aligned}\Delta_L^{(1)W} &= \frac{g^2 m_a}{64\pi^2 m_W^3} \sum_{i=1}^9 U_{ai}^v U_{bi}^{*v} \left\{ m_{n_i}^2 \left(B_0^{(1)} + B_0^{(2)} + B_1^{(1)} \right) + m_b^2 B_1^{(2)} - \left(2m_W^2 + m_{h_1^0}^2 \right) m_{n_i}^2 C_0 \right. \\ &\quad - \left[m_{n_i}^2 \left(2m_W^2 + m_{h_1^0}^2 \right) + 2m_W^2 \left(2m_W^2 + m_a^2 - m_b^2 \right) \right] C_1 \\ &\quad \left. - \left[2m_W^2 \left(m_a^2 - m_{h_1^0}^2 \right) + m_b^2 m_{h_1^0}^2 \right] C_2 \right\}, \\ \Delta_R^{(1)W} &= \frac{g^3 m_b}{64\pi^2 m_W^3} \sum_{i=1}^9 U_{ai}^v U_{bi}^{*v} \left\{ m_{n_i}^2 \left(B_0^{(1)} + B_0^{(2)} + B_1^{(2)} \right) + m_a^2 B_1^{(1)} - \left(2m_W^2 + m_{h_1^0}^2 \right) m_{n_i}^2 C_0 \right. \\ &\quad - \left[m_{n_i}^2 \left(2m_W^2 + m_{h_1^0}^2 \right) + 2m_W^2 \left(2m_W^2 - m_a^2 + m_b^2 \right) \right] C_2 \\ &\quad \left. - \left[2m_W^2 \left(m_b^2 - m_{h_1^0}^2 \right) + m_a^2 m_{h_1^0}^2 \right] C_1 \right\}, \\ \Delta_L^{(7+8)W} &= \frac{g^3 m_a m_b^2}{64\pi^2 m_W^3 (m_b^2 - m_a^2)} \\ &\quad \times \sum_{i=1}^9 U_{ai}^v U_{bi}^{*v} \left[2m_{n_i}^2 \left(B_0^{(2)} - B_0^{(1)} \right) + \left(2m_W^2 + m_{n_i}^2 \right) \left(B_1^{(2)} - B_1^{(1)} \right) + m_b^2 B_1^{(2)} - m_a^2 B_1^{(1)} \right], \\ \Delta_R^{(7+8)W} &= \frac{m_a}{m_b} \Delta_L^{(7+8)W},\end{aligned}$$

where $B_{0,1}^{(k)} = B_{0,1}^{(k)}(m_{n_i}^2, m_W^2)$ and $C_{0,1,2} = C_{0,1,2}(m_{n_i}^2, m_W^2, m_W^2)$,

$$\begin{aligned}\Delta_L^{(5)W} &= \frac{g^3 m_a}{64\pi^2 m_W^3} \sum_{i,j=1}^9 U_{ai}^{v*} U_{bj}^v \left\{ D_{ij} \left[-m_{n_j}^2 B_0^{(12)} + m_{n_i}^2 B_1^{(1)} + m_{n_j}^2 m_W^2 C_0 \right. \right. \\ &\quad + \left(2m_W^2 (m_{n_i}^2 + m_{n_j}^2) + 2m_{n_i}^2 m_{n_j}^2 - m_a^2 m_{n_j}^2 - m_b^2 m_{n_i}^2 \right) C_1 \\ &\quad \left. \left. + D_{ij}^* m_{n_i} m_{n_j} \left[-B_0^{(12)} + B_1^{(1)} + m_W^2 C_0 + \left(4m_W^2 + m_{n_i}^2 + m_{n_j}^2 - m_a^2 - m_b^2 \right) C_1 \right] \right\}, \\ \Delta_R^{(5)W} &= \frac{g^3 m_b}{64\pi^2 m_W^3} \sum_{i,j=1}^9 U_{ai}^{v*} U_{bj}^v \left\{ D_{ij} \left[-m_{n_i}^2 B_0^{(12)} + m_{n_j}^2 B_1^{(2)} + m_{n_i}^2 m_W^2 C_0 \right. \right. \\ &\quad + \left(2m_W^2 (m_{n_i}^2 + m_{n_j}^2) + 2m_{n_i}^2 m_{n_j}^2 - m_a^2 m_{n_j}^2 - m_b^2 m_{n_i}^2 \right) C_2 \\ &\quad \left. \left. + D_{ij}^* m_{n_i} m_{n_j} \left[-B_0^{(12)} + B_1^{(2)} + m_W^2 C_0 + \left(4m_W^2 + m_{n_i}^2 + m_{n_j}^2 - m_a^2 - m_b^2 \right) C_2 \right] \right\},\end{aligned}$$

where $D_{ij} = \sum_{c=1}^3 U_{ci}^v U_{cj}^{*v}$, $B_0^{(12)} = B_0^{(12)}(m_{n_i}^2, m_{n_j}^2)$, $B_1^{(1)} = B_1^{(1)}(m_W^2, m_{n_i}^2)$, $B_1^{(2)} = B_1^{(2)}(m_W^2, m_{n_j}^2)$, and $C_{0,1,2} = C_{0,1,2}(m_W^2, m_{n_i}^2, m_{n_j}^2)$. The analytic expressions $\Delta_{L,R}^{(i)Y} \equiv \Delta_{(ab)L,R}^{(i)Y h_3^\pm}$ with $i = 4, 6, 9, 10$

are

$$\begin{aligned}
\Delta_L^{(1)Y} &= \frac{g^3 m_a c_\beta s_\theta}{64\pi^2 m_Y^3} \sum_{i=1}^9 U_{(a+3)i}^\nu U_{(b+3)i}^{\nu*} \left\{ m_{n_i}^2 \left(B_0^{(1)} + B_0^{(2)} + B_1^{(1)} \right) + m_b^2 B_1^{(2)} \right. \\
&\quad - \left(2m_Y^2 + m_{h_1^0}^2 \right) m_{n_i}^2 C_0 - \left[2m_Y^2 (2m_Y^2 + m_a^2 - m_b^2) + m_{n_i}^2 (2m_Y^2 + m_{h_1^0}^2) \right] C_1 \\
&\quad \left. + \left[2m_Y^2 (m_a^2 - m_{h_1^0}^2) + m_b^2 m_{h_1^0}^2 \right] C_2 \right\}, \\
\Delta_R^{(1)Y} &= \frac{g^3 m_b c_\beta s_\theta}{64\pi^2 m_Y^3} \sum_{i=1}^9 U_{(a+3)i}^{\nu*} U_{(b+3)i}^\nu \left\{ m_{n_i}^2 \left(B_0^{(1)} + B_0^{(2)} + B_1^{(2)} \right) + m_a^2 B_1^{(1)} \right. \\
&\quad - \left(2m_Y^2 + m_{h_1^0}^2 \right) m_{n_i}^2 C_0 - \left[2m_Y^2 (2m_Y^2 - m_a^2 + m_b^2) + m_{n_i}^2 (2m_Y^2 + m_{h_1^0}^2) \right] C_2 \\
&\quad \left. + \left[2m_Y^2 (m_b^2 - m_{h_1^0}^2) + m_b^2 m_{h_1^0}^2 \right] C_1 \right\}, \\
\Delta_L^{(7+8)Y} &= \frac{g^3 m_a m_b^2}{64\pi^2 m_W m_Y^2 (m_b^2 - m_a^2)} \sum_{i=1}^9 U_{(a+3)i}^{\nu*} U_{(b+3)i}^\nu \\
&\quad \times \left[2m_{n_i}^2 \left(B_0^{(2)} - B_0^{(1)} \right) + (2m_Y^2 + m_{n_i}^2) \left(B_1^{(2)} - B_1^{(1)} \right) - m_a^2 B_1^{(1)} + m_b^2 B_1^{(2)} \right], \\
\Delta_R^{(7+8)Y} &= \frac{m_a}{m_b} \Delta_L^{(7+8)Y},
\end{aligned}$$

where $B_{0,1}^{(k)} = B_{0,1}^{(k)}(m_{n_i}^2, m_Y^2)$ and $C_{0,1,2} = C_{0,1,2}(m_{n_i}^2, m_Y^2, m_Y^2)$. One-loop contributions from diagram (5) are

$$\begin{aligned}
\Delta_L^{(5)Y} &= \frac{g^3 m_a}{64\pi^2 m_W m_Y^2} \\
&\quad \times \sum_{i,j=1}^9 U_{(a+3)i}^\nu U_{(b+3)j}^{\nu*} \left\{ D_{ij} \left[-m_{n_j}^2 B_0^{(12)} + m_{n_i}^2 B_1^{(1)} + m_{n_j}^2 m_W^2 C_0 \right. \right. \\
&\quad + \left(2m_W^2 (m_{n_i}^2 + m_{n_j}^2) + 2m_{n_i}^2 m_{n_j}^2 - m_a^2 m_{n_j}^2 - m_b^2 m_{n_i}^2 \right) C_1 \\
&\quad \left. \left. + D_{ij}^* m_{n_i} m_{n_j} \left[-B_0^{(12)} + B_1^{(1)} + m_W^2 C_0 + \left(4m_W^2 + m_{n_i}^2 + m_{n_j}^2 - m_a^2 - m_b^2 \right) C_1 \right] \right\}, \\
\Delta_R^{(5)Y} &= \frac{g^3 m_b}{64\pi^2 m_W m_Y^2} \\
&\quad \times \sum_{i,j=1}^9 U_{(a+3)i}^\nu U_{(b+3)j}^{\nu*} \left\{ D_{ij} \left[-m_{n_i}^2 B_0^{(12)} + m_{n_j}^2 B_1^{(2)} + m_{n_i}^2 m_W^2 C_0 \right. \right. \\
&\quad + \left(2m_W^2 (m_{n_i}^2 + m_{n_j}^2) + 2m_{n_i}^2 m_{n_j}^2 - m_a^2 m_{n_j}^2 - m_b^2 m_{n_i}^2 \right) C_2 \\
&\quad \left. \left. + D_{ij}^* m_{n_i} m_{n_j} \left[-B_0^{(12)} + B_1^{(2)} + m_W^2 C_0 + \left(4m_W^2 + m_{n_i}^2 + m_{n_j}^2 - m_a^2 - m_b^2 \right) C_2 \right] \right\},
\end{aligned}$$

where $B_0^{(12)} = B_0^{(12)}(m_{n_i}^2, m_{n_j}^2)$, $B_1^{(1)} = B_1^{(1)}(m_Y^2, m_{n_i}^2)$, $B_1^{(2)} = B_1^{(2)}(m_Y^2, m_{n_j}^2)$, and $C_{0,1,2} = C_{0,1,2}(m_Y^2, m_{n_i}^2, m_{n_j}^2)$,

$$\begin{aligned}\Delta_L^{(2)Y} &= -\frac{g^3 m_a c_\theta c_\beta}{64\pi^2 m_W m_Y^2} \sum_{i=1}^9 U_{(a+3)i}^\nu \\ &\times \left\{ \lambda_{bi}^{L,1} m_{n_i} \left[B_0^{(1)} + B_1^{(1)} + (m_Y^2 + m_{h_3^\pm}^2 - m_{h_1^0}^2) C_0 - (m_Y^2 - m_{h_3^\pm}^2 + m_{h_1^0}^2) C_1 \right] \right. \\ &\quad \left. - \lambda_{bi}^{R,1} m_b \left[2m_Y^2 C_1 + (m_Y^2 + m_{h_3^\pm}^2 - m_{h_1^0}^2) C_2 \right] \right\}, \\ \Delta_R^{(2)Y} &= \frac{g^3 c_\theta c_\beta}{64\pi^2 m_W m_Y^2} \sum_{i=1}^9 U_{(a+3)i}^\nu \\ &\times \left\{ \lambda_{bi}^{L,1} m_b m_{n_i} \left[2m_Y^2 C_0 + (m_Y^2 - m_{h_3^\pm}^2 + m_{h_1^0}^2) C_2 \right] \right. \\ &\quad + \lambda_{bi}^{R,1} \left[m_{n_i}^2 B_0^{(1)} + m_a^2 B_1^{(1)} - m_{n_i}^2 (m_Y^2 - m_{h_3^\pm}^2 + m_{h_1^0}^2) C_0 \right. \\ &\quad \left. \left. + \left[2m_Y^2 (m_{h_1^0}^2 - m_b^2) - m_a^2 (m_Y^2 - m_{h_3^\pm}^2 + m_{h_1^0}^2) \right] C_1 - 2m_b^2 m_Y^2 C_2 \right] \right\},\end{aligned}$$

where $B_k^{(1)} = B_k^{(1)}(m_Y^2, m_{n_i}^2)$ ($k = 0, 1$) and $C_{0,1,2} = C_{0,1,2}(m_{n_i}^2, m_Y^2 m_{h_3^\pm}^2)$,

$$\begin{aligned}\Delta_L^{(3)Y} &= \frac{g^3 c_\theta c_\beta}{64\pi^2 m_W m_Y^2} \sum_{i=1}^9 U_{(b+3)i}^{\nu*} \\ &\times \left\{ \lambda_{ai}^{L,1*} m_a m_{n_i} \left[2m_Y^2 C_0 + (m_Y^2 - m_{h_3^\pm}^2 + m_{h_1^0}^2) C_1 \right] \right. \\ &\quad + \lambda_{ai}^{R,1*} \left[m_{n_i}^2 B_0^{(2)} + m_b^2 B_1^{(2)} - m_{n_i}^2 (m_Y^2 - m_{h_3^\pm}^2 + m_{h_1^0}^2) C_0 \right. \\ &\quad \left. \left. - 2m_a^2 m_Y^2 C_1 + \left[2m_Y^2 (m_{h_1^0}^2 - m_a^2) - m_b^2 (m_Y^2 - m_{h_3^\pm}^2 + m_{h_1^0}^2) \right] C_2 \right] \right\}, \\ \Delta_R^{(3)Y} &= -\frac{g^3 m_b c_\theta c_\beta}{64\pi^2 m_W m_Y^2} \\ &\times \sum_{i=1}^9 U_{(b+3)i}^{\nu*} \left\{ \lambda_{ai}^{L,1*} m_{n_i} \left[B_0^{(2)} + B_1^{(2)} + (m_Y^2 + m_{h_3^\pm}^2 - m_{h_1^0}^2) C_0 - (m_Y^2 - m_{h_3^\pm}^2 + m_{h_1^0}^2) C_2 \right] \right. \\ &\quad \left. - \lambda_{ai}^{R,1*} m_a \left[(m_Y^2 + m_{h_3^\pm}^2 - m_{h_1^0}^2) C_1 + 2m_Y^2 C_2 \right] \right\},\end{aligned}$$

where $B_k^{(2)} = B_k^{(2)}(m_Y^2, m_{n_i}^2)$ and $C_{0,1,2} = C_{0,1,2}(m_{n_i}^2, m_{h_3^\pm}^2, m_Y^2)$,

$$\begin{aligned}\Delta_L^{(4)h_{k,l}^\pm} &= \frac{g^2 g_{hkl}}{32\pi^2 m_W^2} \sum_{i=1}^9 \left[-\lambda_{ai}^{R,k*} \lambda_{bi}^{L,k} m_{n_i} C_0 + \lambda_{ai}^{L,k*} \lambda_{bi}^{L,k} m_a C_1 + \lambda_{ai}^{R,k*} \lambda_{bi}^{R,k} m_b C_2 \right], \\ \Delta_R^{(4)h_{k,l}^\pm} &= \frac{g^2 g_{hkl}}{32\pi^2 m_W^2} \sum_{i=1}^9 \left[-\lambda_{ai}^{L,k*} \lambda_{bi}^{R,k} m_{n_i} C_0 + \lambda_{ai}^{R,k*} \lambda_{bi}^{R,k} m_a C_1 + \lambda_{ai}^{L,k*} \lambda_{bi}^{L,k} m_b C_2 \right],\end{aligned}$$

where $\{k, l\} = \{1, 2\}, \{2, 1\}, \{1, 1\}, \{2, 2\}, \{3, 3\}$, $g_{h21} = g_{h12}$, and $C_{0,1,2} = C_{0,1,2}(m_{n_i}^2, m_{h_k^\pm}^2, m_{h_l^\pm}^2)$,

$$\begin{aligned}\Delta_L^{(6)h_k^\pm} &= \frac{g^3}{64\pi^2 m_W^3} \sum_{i,j=1}^9 \left\{ \lambda_{ij}^{0*} \left[\lambda_{ai}^{R,k*} \lambda_{bj}^{L,k} \left(B_0^{(12)} + m_{h_k^\pm}^2 C_0 + m_a^2 C_1 + m_b^2 C_2 \right) \right. \right. \\ &\quad + \lambda_{ai}^{R,k*} \lambda_{bj}^{R,k} m_b m_{n_j} C_2 + \lambda_{ai}^{L,k*} \lambda_{bj}^{L,k} m_a m_{n_i} C_1 \Big] \\ &\quad + \lambda_{ij}^0 \left[\lambda_{ai}^{R,k*} \lambda_{bj}^{L,k} m_{n_i} m_{n_j} C_0 + \lambda_{ai}^{R,k*} \lambda_{bj}^{R,k} m_{n_i} m_b (C_0 + C_2) \right. \\ &\quad \left. \left. + \lambda_{ai}^{L,k*} \lambda_{bj}^{L,k} m_a m_{n_j} (C_0 + C_1) + \lambda_{ai}^{L,k*} \lambda_{bj}^{R,k} m_a m_b (C_0 + C_1 + C_2) \right] \right\}, \\ \Delta_R^{(6)h_k^\pm} &= \frac{g^3}{64\pi^2 m_W^3} \sum_{i,j=1}^9 \left\{ \lambda_{ij}^0 \left[\lambda_{ai}^{L,k*} \lambda_{bj}^{R,k} \left(B_0^{(12)} + m_{h_k^\pm}^2 C_0 + m_a^2 C_1 + m_b^2 C_2 \right) \right. \right. \\ &\quad + \lambda_{ai}^{L,k*} \lambda_{bj}^{L,k} m_b m_{n_j} C_2 + \lambda_{ai}^{R,k*} \lambda_{bj}^{R,k} m_a m_{n_i} C_1 \Big] \\ &\quad + \lambda_{ij}^{0*} \left[\lambda_{ai}^{L,k*} \lambda_{bj}^{R,k} m_{n_i} m_{n_j} C_0 + \lambda_{ai}^{L,k*} \lambda_{bj}^{L,k} m_{n_i} m_b (C_0 + C_2) \right. \\ &\quad \left. \left. + \lambda_{ai}^{R,k*} \lambda_{bj}^{R,k} m_a m_{n_j} (C_0 + C_1) + \lambda_{ai}^{R,k*} \lambda_{bj}^{L,k} m_a m_b (C_0 + C_1 + C_2) \right] \right\},\end{aligned}$$

where $k = 1, 2, 3$, $B_0^{(12)} = B_0^{(12)}(m_{n_i}^2, m_{n_j}^2)$, and $C_{0,1,2} = C_{0,1,2}(m_{n_i}^2, m_{n_j}^2, m_{h_k^\pm}^2)$,

$$\begin{aligned}\Delta_L^{(9+10)h_k^\pm} &= \frac{g^3}{64\pi^2 m_W^3 (m_a^2 - m_b^2)} \\ &\times \sum_{i=1}^9 \left[m_a m_b m_{n_i} \lambda_{ai}^{L,k*} \lambda_{bi}^{R,k} \left(B_0^{(1)} - B_0^{(2)} \right) + m_{n_i} \lambda_{ai}^{R,k*} \lambda_{bi}^{L,k} \left(m_b^2 B_0^{(1)} - m_a^2 B_0^{(2)} \right) \right. \\ &\quad \left. + m_a m_b \left(\lambda_{ai}^{L,k*} \lambda_{bi}^{L,k} m_b + \lambda_{ai}^{R,k*} \lambda_{bi}^{R,k} m_a \right) \left(-B_1^{(1)} + B_1^{(2)} \right) \right], \\ \Delta_R^{(9+10)h_k^\pm} &= \frac{g^3}{64\pi^2 m_W^3 (m_a^2 - m_b^2)} \\ &\times \sum_{i=1}^9 \left[m_a m_b m_{n_i} \lambda_{ai}^{R,k*} \lambda_{bi}^{L,k} \left(B_0^{(1)} - B_0^{(2)} \right) + m_{n_i} \lambda_{ai}^{L,k*} \lambda_{bi}^{R,k} \left(m_b^2 B_0^{(1)} - m_a^2 B_0^{(2)} \right) \right. \\ &\quad \left. + m_a m_b \left(\lambda_{ai}^{R,k*} \lambda_{bi}^{R,k} m_b + \lambda_{ai}^{L,k*} \lambda_{bi}^{L,k} m_a \right) \left(-B_1^{(1)} + B_1^{(2)} \right) \right],\end{aligned}$$

where $k = 1, 2, 3$, $B_{0,1}^{(k)} = B_{0,1}^{(k)}(m_{n_i}^2, m_{h_k^\pm}^2)$. The details for deriving the above formulas of $\Delta_{L,R}^{(i)}$ were shown in Refs. [25, 121], and hence we do not present them in this work. We note that the scalar functions $\Delta_{L,R}^{(1)W}$ and $\Delta_{L,R}^{(1,2,3)Y}$ include parts that do not depend on m_{n_i} , and therefore they vanish because of the Glashow–Iliopoulos–Maiani mechanism.

The divergent cancellation in the total $\Delta_{L,R}$ is shown as follows:

$$\begin{aligned}
\text{div} \left[\Delta_L^{(1)W} \right] &= m_a \Delta_\epsilon \times \frac{3}{2} \times \sum_{i=1}^9 U_{ai}^{v*} U_{bi}^v m_{n_i}^2, \\
\text{div} \left[\Delta_L^{(5)W} \right] &= m_a \Delta_\epsilon \times \sum_{i,j=1}^9 U_{ai}^{v*} U_{bj}^v \left(-D_{ij}^* m_{n_j}^2 - \frac{1}{2} D_{ij} m_{n_i}^2 \right), \\
\text{div} \left[\Delta_L^{(7+8)W} \right] &= \text{div} \left[\Delta_L^{(4)Y} \right] = \text{div} \left[\Delta_L^{(7+8)Y} \right] = 0, \\
\text{div} \left[\Delta_L^{(1)Y} \right] &= m_a \Delta_\epsilon \times \left(\frac{3s_\theta^4}{2c_\beta^2} \right) \sum_{i=1}^9 U_{(a+3)i}^v U_{(b+3)i}^v m_{n_i}^2, \\
\text{div} \left[\Delta_L^{(2)Y} \right] &= m_a \Delta_\epsilon \times \left(-\frac{c_\theta s_\theta^2}{2c_\beta} \right) \sum_{i=1}^9 U_{(a+3)i}^v \lambda_{bi}^{L,1} m_{n_i}, \\
\text{div} \left[\Delta_L^{(3)Y} \right] &= \Delta_\epsilon \times \left(\frac{c_\theta s_\theta^2}{c_\beta} \right) \sum_{i=1}^9 U_{(a+3)i}^v L_{ai}^{R,1} m_{n_i}^2, \\
\text{div} \left[\Delta_L^{(5)Y} \right] &= m_a \Delta_\epsilon \times \frac{s_\theta^2}{c_\beta^2} \sum_{i,j=1}^9 U_{(a+3)i}^{v*} U_{(b+3)j}^v \left(-D_{ij}^* m_{n_j}^2 - \frac{1}{2} D_{ij} m_{n_i}^2 \right), \\
\text{div} \left[\Delta_L^{(6)Yh_k^\pm} \right] &= m_a \Delta_\epsilon \times \sum_{i,j=1}^9 U_{(a+3)i}^{v*} \lambda_{ij}^{0*} \lambda_{bj}^{L,k}, \\
\text{div} \left[\Delta_L^{(9+10)Yh_k^\pm} \right] &= -m_a \Delta_\epsilon \times \sum_{i=1}^9 U_{(a+3)i}^{v*} \lambda_{bi}^{L,k} m_{n_i}, \tag{A1}
\end{aligned}$$

where $\text{div}B_0^{(1)} = \text{div}B_0^{(2)} = \text{div}B_0^{(12)} = -2\text{div}B_1^{(1)} = -2\text{div}B_1^{(2)} = \Delta_\epsilon$ and $1/m_Y = s_\theta/(c_\beta m_W)$.

It is easy to see that $\text{div} \left[\Delta_L^{(1)W} \right] + \text{div} \left[\Delta_L^{(5)W} \right] = \text{div} \left[\Delta_L^{(6)Yh_k^\pm} \right] + \text{div} \left[\Delta_L^{(9+10)Yh_k^\pm} \right] = 0$ and the sum of the remaining divergent parts is zero in the case we are focusing on investigating: $c_\theta = 1$.

REFERENCES

- [1] Y. Fukuda[Super-Kamiokande Collaboration] et al. [Super-Kamiokande Collaboration], Phys. Rev. Lett. **81**, 1562 (1998) [[arXiv:hep-ex/9807003Search inSPIRE](#)].
- [2] S. Fukuda[Super-Kamiokande Collaboration] et al. [Super-Kamiokande Collaboration], Phys. Rev. Lett. **86**, 5651 (2001) [[arXiv:hep-ex/0103032Search inSPIRE](#)].
- [3] S. Fukuda[Super-Kamiokande Collaboration] et al. [Super-Kamiokande Collaboration], Phys. Rev. Lett. **86**, 5656 (2001) [[arXiv:hep-ex/0103033Search inSPIRE](#)].
- [4] Q. R. Ahmad[SNO Collaboration] et al. [SNO Collaboration], Phys. Rev. Lett. **89**, 011301 (2002) [[arXiv:nucl-ex/0204008Search inSPIRE](#)].
- [5] Q. R. Ahmad[SNO Collaboration] et al. [SNO Collaboration], Phys. Rev. Lett. **89**, 011302 (2002) [[arXiv:nucl-ex/0204009Search inSPIRE](#)].
- [6] B. Aubert[BaBar Collaboration] et al. [BaBar Collaboration], Phys. Rev. Lett. **104**, 021802 (2010) [[arXiv:0908.2381 \[hep-ex\]Search inSPIRE](#)].
- [7] A. M. Baldini[MEG Collaboration] et al. [MEG Collaboration], Eur. Phys. J. C **76**, 434 (2016) [[arXiv:1605.05081 \[hep-ex\]Search inSPIRE](#)].
- [8] E. Kou[Belle-II Collaboration] et al. [Belle-II Collaboration], Prog. Theor. Exp. Phys. **2019**, 123C01 (2019); **2020**, 029201 (2020) [erratum] [[arXiv:1808.10567 \[hep-ex\]Search inSPIRE](#)].

- [9] T. Aushev, et al., [arXiv:1002.5012 \[hep-ex\]](#)[Search inSPIRE](#).
- [10] A. M. Baldini[MEG II Collaboration] et al. [MEG II Collaboration], Eur. Phys. J. C **78**, 380 (2018) [[arXiv:1801.04688 \[physics.ins-det\]](#)[Search inSPIRE](#)].
- [11] A. M. Sirunyan[CMS Collaboration] et al. [CMS Collaboration], J. High Energy Phys. **06**, 001 (2018).
- [12] G. Aad[ATLAS Collaboration] et al. [ATLAS Collaboration], Phys. Lett. B **800**, 135069 (2020) [[arXiv:1907.06131 \[hep-ex\]](#)[Search inSPIRE](#)].
- [13] ATLAS Collaboration, ATLAS-CONF-2019-037, in Proc. 29th Int. Symp. Lepton Photon Interactions at High Energies .
- [14] Q. Qin, Q. Li, C. D. Lü, F. S. Yu, and S. H. Zhou, Eur. Phys. J. C **78** 835 (2018) [[arXiv:1711.07243 \[hep-ph\]](#)[Search inSPIRE](#)].
- [15] A. Zee, Phys. Lett. B **93**, 389 (1980); **95**, 461 (1980) [erratum].
- [16] R. K. Barman, R. Dcruz, and A. Thapa, J. High Energy Phys. **03**, 183 (2022) [[arXiv:2112.04523 \[hep-ph\]](#)[Search inSPIRE](#)].
- [17] J. Herrero-García, T. Ohlsson, S. Riad, and J. Wirén, J. High Energy Phys. **04**, 130 (2017).
- [18] D. Sabatta, A. S. Cornell, A. Goyal, M. Kumar, B. Mellado, and X. Ruan, Chin. Phys. C **44**, 063103 (2020) [[arXiv:1909.03969 \[hep-ph\]](#)[Search inSPIRE](#)].
- [19] A. Vicente, Front. Phys. **7**, 174 (2019) [[arXiv:1908.07759 \[hep-ph\]](#)[Search inSPIRE](#)].
- [20] E. Arganda, A. M. Curiel, M. J. Herrero, and D. Temes, Phys. Rev. D **71**, 035011 (2005).
- [21] X. Marcano and R. A. Morales, Front. Phys. **7**, 228 (2020) [[arXiv:1909.05888 \[hep-ph\]](#)[Search inSPIRE](#)].
- [22] A. Ilakovac, Phys. Rev. D **62**, 036010 (2000).
- [23] E. Arganda, M. J. Herrero, X. Marcano, and C. Weiland, Phys. Rev. D **91**, 015001 (2015).
- [24] E. Arganda, M. J. Herrero, X. Marcano, R. Morales, and A. Szynkman, Phys. Rev. D **95**, 095029 (2017).
- [25] N. H. Thao, L. T. Hue, H. T. Hung, and N. T. Xuan, Nucl. Phys. B **921**, 159 (2017) [[arXiv:1703.00896 \[hep-ph\]](#)[Search inSPIRE](#)].
- [26] G. Hernández-Tomé, J. I. Illana, and M. Masip, Phys. Rev. D **102**, 113006 (2020) [[arXiv:2005.11234 \[hep-ph\]](#)[Search inSPIRE](#)].
- [27] T. P. Nguyen, T. T. Thuc, D. T. Si, T. T. Hong, and L. T. Hue, Prog. Theor. Exp. Phys. **2022**, 023 (2022) [[arXiv:2011.12181 \[hep-ph\]](#)[Search inSPIRE](#)].
- [28] A. Brignole and A. Rossi, Phys. Lett. B **566**, 217 (2003).
- [29] A. Brignole and A. Rossi, Nucl. Phys. B **701**, 3 (2004).
- [30] J. L. Diaz-Cruz, J. High Energy Phys. **05**, 036 (2003).
- [31] P. T. Giang, L. T. Hue, D. T. Huong, and H. N. Long, Nucl. Phys. B **864**, 85 (2012).
- [32] M. Arana-Catania, E. Arganda, and M. J. Herrero, J. High Energy Phys. **09**, 160 (2013); **10**, 192 (2015) [erratum].
- [33] L. T. Hue, H. N. Long, T. T. Thuc, and T. Phong Nguyen, Nucl. Phys. B **07**, 37 (2016) [[arXiv:1512.03266 \[hep-ph\]](#)[Search inSPIRE](#)].
- [34] E. Arganda, M. J. Herrero, R. Morales, and A. Szynkman, J. High Energy Phys. **03**, 055 (2016).
- [35] E. Arganda, M. J. Herrero, X. Marcano, and C. Weiland, Phys. Rev. D **93**, 055010 (2016).
- [36] M. Zeleny-Mora, J. L. Díaz-Cruz, and O. Félix-Beltrán; [arXiv:2112.08412 \[hep-ph\]](#)[Search inSPIRE](#).
- [37] B. Yang, J. Han, and N. Liu, Phys. Rev. D **95**, 035010 (2017).
- [38] H. K. Guo, Y. Y. Li, T. Liu, M. Ramsey-Musolf, and J. Shu, Phys. Rev. D **96**, 115034 (2017).
- [39] M. Aoki, S. Kanemura, K. Sakurai, and H. Sugiyama, Phys. Lett. B **763**, 352 (2016).
- [40] K. Cheung, W. Y. Keung, and P. Y. Tseng, Phys. Rev. D **93**, 015010 (2016).
- [41] K. Huitu, V. Keus, N. Koivunen, and O. Lebedev, J. High Energy Phys. **05**, 026 (2016).
- [42] C. H. Chen and T. Nomura, Eur. Phys. J. C **76**, 353 (2016).
- [43] C. F. Chang, C. H. V. Chang, C. S. Nugroho, and T. C. Yuan, Nucl. Phys. B **910**, 293 (2016).
- [44] W. Altmannshofer, S. Gori, A. L. Kagan, L. Silvestrini, and J. Zupan, Phys. Rev. D **93**, 031301 (2016).
- [45] Y. Omura, E. Senaha, and K. Tobe, Phys. Rev. D **94**, 055019 (2016).
- [46] A. Lami and P. Roig, Phys. Rev. D **94**, 056001 (2016).
- [47] D. Das and A. Kundu, Phys. Rev. D **92**, 015009 (2015).
- [48] A. Crivellin, G. D'Ambrosio, and J. Heeck, Phys. Rev. Lett. **114**, 151801 (2015).

- [49] M. D. Campos, A. E. Cárcamo Hernández, H. Päs, and E. Schumacher, Phys. Rev. D **91**, 116011 (2015).
- [50] Y. Omura, E. Senaha, and K. Tobe, J. High Energy Phys. **05**, 028 (2015).
- [51] L. de Lima, C. S. Machado, R. D. Matheus, and L. A. F. do Prado, J. High Energy Phys. **11**, 074 (2015).
- [52] J. Heeck, M. Holthausen, W. Rodejohann, and Y. Shimizu, Nucl. Phys. B **896**, 281 (2015).
- [53] I. Doršner, S. Fajfer, A. Greljo, J. F. Kamenik, N. Košnik, and I. Nišandžić, J. High Energy Phys. **06**, 108 (2015).
- [54] X. G. He, J. Tandean, and Y. J. Zheng, J. High Energy Phys. **09**, 093 (2015).
- [55] A. Dery, A. Efrati, Y. Nir, Y. Soreq, and V. Susič, Phys. Rev. D **90**, 115022 (2014).
- [56] A. Celis, V. Cirigliano, and E. Passemar, Phys. Rev. D **89**, 013008 (2014).
- [57] A. Falkowski, D. M. Straub, and A. Vicente, J. High Energy Phys. **05**, 092 (2014).
- [58] R. Harnik, J. Kopp, and J. Zupan, J. High Energy Phys. **03**, 026 (2013).
- [59] P. S. Bhupal Dev, R. Franceschini, and R. N. Mohapatra, Phys. Rev. D **86**, 093010 (2012).
- [60] A. Goudelis, O. Lebedev, and J. H. Park, Phys. Lett. B **707**, 369 (2012).
- [61] J. L. Diaz-Cruz and J. J. Toscano, Phys. Rev. D **62**, 116005 (2000).
- [62] J. G. Korner, A. Pilaftsis, and K. Schilcher, Phys. Rev. D **47**, 1080 (1993).
- [63] A. Pilaftsis, Z. Phys. C **55**, 275 (1992).
- [64] A. Pilaftsis, Phys. Lett. B **285**, 68 (1992).
- [65] G. Blankenburg, J. Ellis, and G. Isidori, Phys. Lett. B **712**, 386 (2012).
- [66] A. E. Cárcamo Hernández, E. Cataño Mur, and R. Martínez, Phys. Rev. D **90**, 073001 (2014) [[arXiv:1407.5217 \[hep-ph\]](#)]Search inSPIRE].
- [67] D. Jurčiukonis and L. Lavoura, J. High Energy Phys. **03**, 106 (2022) [[arXiv:2107.14207 \[hep-ph\]](#)]Search inSPIRE].
- [68] T. Aoyama, et al. Phys. Rep. **887**, 1 (2020) [[arXiv:2006.04822 \[hep-ph\]](#)]Search inSPIRE].
- [69] T. Aoyama, M. Hayakawa, T. Kinoshita, and M. Nio, Phys. Rev. Lett. **109**, 111808 (2012) [[arXiv:1205.5370 \[hep-ph\]](#)]Search inSPIRE].
- [70] T. Aoyama, T. Kinoshita, and M. Nio, Atoms **7**, 28 (2019).
- [71] A. Czarnecki, W. J. Marciano, and A. Vainshtein, Phys. Rev. D **67**, 073006 (2003); **73**, 119901 (2006) [erratum] [[arXiv:hep-ph/0212229](#)]Search inSPIRE].
- [72] C. Gnendiger, D. Stöckinger, and H. Stöckinger-Kim, Phys. Rev. D **88**, 053005 (2013) [[arXiv:1306.5546 \[hep-ph\]](#)]Search inSPIRE].
- [73] M. Davier, A. Hoecker, B. Malaescu, and Z. Zhang, Eur. Phys. J. C **77**, 827 (2017) [[arXiv:1706.09436 \[hep-ph\]](#)]Search inSPIRE].
- [74] A. Keshavarzi, D. Nomura, and T. Teubner, Phys. Rev. D **97**, 114025 (2018) [[arXiv:1802.02995 \[hep-ph\]](#)]Search inSPIRE].
- [75] G. Colangelo, M. Hoferichter, and P. Stoffer, J. High Energy Phys. **02**, 006 (2019) [[arXiv:1810.00007 \[hep-ph\]](#)]Search inSPIRE].
- [76] M. Hoferichter, B. L. Hoid, and B. Kubis, J. High Energy Phys. **08**, 137 (2019) [[arXiv:1907.01556 \[hep-ph\]](#)]Search inSPIRE].
- [77] M. Davier, A. Hoecker, B. Malaescu, and Z. Zhang, Eur. Phys. J. C **80**, 241 (2020); **80**, 410 (2020) [erratum] [[arXiv:1908.00921 \[hep-ph\]](#)]Search inSPIRE].
- [78] A. Keshavarzi, D. Nomura, and T. Teubner, Phys. Rev. D **101**, 014029 (2020) [[arXiv:1911.00367 \[hep-ph\]](#)]Search inSPIRE].
- [79] A. Kurz, T. Liu, P. Marquard, and M. Steinhauser, Phys. Lett. B **734**, 144 (2014) [[arXiv:1403.6400 \[hep-ph\]](#)]Search inSPIRE].
- [80] K. Melnikov and A. Vainshtein, Phys. Rev. D **70**, 113006 (2004) [[arXiv:hep-ph/0312226](#)]Search inSPIRE].
- [81] P. Masjuan and P. Sanchez-Puertas, Phys. Rev. D **95**, 054026 (2017) [[arXiv:1701.05829 \[hep-ph\]](#)]Search inSPIRE].
- [82] G. Colangelo, M. Hoferichter, M. Procura, and P. Stoffer, J. High Energy Phys. **04**, 161 (2017) [[arXiv:1702.07347 \[hep-ph\]](#)]Search inSPIRE].
- [83] M. Hoferichter, B. L. Hoid, B. Kubis, S. Leupold, and S. P. Schneider, J. High Energy Phys. **10**, 141 (2018) [[arXiv:1808.04823 \[hep-ph\]](#)]Search inSPIRE].
- [84] A. Gérardin, H. B. Meyer, and A. Nyffeler, Phys. Rev. D **100**, 034520 (2019) [[arXiv:1903.09471 \[hep-lat\]](#)]Search inSPIRE].

- [85] J. Bijnens, N. Hermansson-Truedsson, and A. Rodríguez-Sánchez, Phys. Lett. B **798**, 134994 (2019) [[arXiv:1908.03331 \[hep-ph\]](#)[Search inSPIRE](#)].
- [86] G. Colangelo, F. Hagelstein, M. Hoferichter, L. Laub, and P. Stoffer, J. High Energy Phys. **03**, 101 (2020) [[arXiv:1910.13432 \[hep-ph\]](#)[Search inSPIRE](#)].
- [87] T. Blum, N. Christ, M. Hayakawa, T. Izubuchi, L. Jin, C. Jung, and C. Lehner, Phys. Rev. Lett. **124**, 132002 (2020) [[arXiv:1911.08123 \[hep-lat\]](#)[Search inSPIRE](#)].
- [88] G. Colangelo, M. Hoferichter, A. Nyffeler, M. Passera, and P. Stoffer, Phys. Lett. B **735**, 90–91 (2014) [[arXiv:1403.7512 \[hep-ph\]](#)[Search inSPIRE](#)].
- [89] V. Pauk and M. Vanderhaeghen, Eur. Phys. J. C **74**, 3008 (2014) [[arXiv:1401.0832 \[hep-ph\]](#)[Search inSPIRE](#)].
- [90] I. Danilkin and M. Vanderhaeghen, Phys. Rev. D **95**, 014019 (2017) [[arXiv:1611.04646 \[hep-ph\]](#)[Search inSPIRE](#)].
- [91] F. Jegerlehner, The Anomalous Magnetic Moment of the Muon (Springer, New York, 2017).
- [92] M. Knecht, S. Narison, A. Rabemananjara, and D. Rabetiarivony, Phys. Lett. B **787**, 111 (2018) [[arXiv:1808.03848 \[hep-ph\]](#)[Search inSPIRE](#)].
- [93] G. Eichmann, C. S. Fischer, and R. Williams, Phys. Rev. D **101**, 054015 (2020) [[arXiv:1910.06795 \[hep-ph\]](#)[Search inSPIRE](#)].
- [94] P. Roig and P. Sanchez-Puertas, Phys. Rev. D **101**, 074019 (2020) [[arXiv:1910.02881 \[hep-ph\]](#)[Search inSPIRE](#)].
- [95] B. Abi[Muon g-2 Collaboration] et al. [Muon g-2 Collaboration], Phys. Rev. Lett. **126**, 141801 (2021) [[arXiv:2104.03281 \[hep-ex\]](#)[Search inSPIRE](#)].
- [96] G. W. Bennett[Muon g-2 Collaboration] et al. [Muon g-2 Collaboration], Phys. Rev. D **73**, 072003 (2006) [[arXiv:hep-ex/0602035](#)[Search inSPIRE](#)].
- [97] S. Borsanyi, et al. Nature **593**, 51 (2021) [[arXiv:2002.12347 \[hep-lat\]](#)[Search inSPIRE](#)].
- [98] A. Crivellin, M. Hoferichter, C. A. Manzari, and M. Montull, Phys. Rev. Lett. **125**, 091801 (2020) [[arXiv:2003.04886 \[hep-ph\]](#)[Search inSPIRE](#)].
- [99] A. Keshavarzi, W. J. Marciano, M. Passera, and A. Sirlin, Phys. Rev. D **102**, 033002 (2020) [[arXiv:2006.12666 \[hep-ph\]](#)[Search inSPIRE](#)].
- [100] G. Colangelo, M. Hoferichter, and P. Stoffer, Phys. Lett. B **814**, 136073 (2021) [[arXiv:2010.07943 \[hep-ph\]](#)[Search inSPIRE](#)].
- [101] L. Morel, Z. Yao, P. Cladé, and S. Guellati-Khélifa, Nature **588**, 61 (2020).
- [102] Z. N. Zhang, H. B. Zhang, J. L. Yang, S. M. Zhao, and T. F. Feng, Phys. Rev. D **103**, 115015 (2021) [[arXiv:2105.09799 \[hep-ph\]](#)[Search inSPIRE](#)].
- [103] S. Baek and K. Nishiwaki, Phys. Rev. D **93**, 015002 (2016) [[arXiv:1509.07410 \[hep-ph\]](#)[Search inSPIRE](#)].
- [104] R. Foot, H. N. Long, and T. A. Tran, Phys. Rev. D **50**, R34 (1994) [[arXiv:hep-ph/9402243](#)[Search inSPIRE](#)].
- [105] H. N. Long, Phys. Rev. D **54**, 4691 (1996) [[arXiv:hep-ph/9607439](#)[Search inSPIRE](#)].
- [106] H. N. Long, Phys. Rev. D **53**, 437 (1996) [[arXiv:hep-ph/9504274](#)[Search inSPIRE](#)].
- [107] L. T. Hue, H. T. Hung, N. T. Tham, H. N. Long, and T. P. Nguyen, Phys. Rev. D **104**, 033007 (2021) [[arXiv:2104.01840 \[hep-ph\]](#)[Search inSPIRE](#)].
- [108] H. B. Zhang, T. F. Feng, S. M. Zhao, Y. L. Yan, and F. Sun, Chin. Phys. C **41**, 043106 (2017) [[arXiv:1511.08979 \[hep-ph\]](#)[Search inSPIRE](#)].
- [109] T. P. Nguyen, T. T. Le, T. T. Hong, and L. T. Hue, Phys. Rev. D **97**, 073003 (2018) [[arXiv:1802.00429 \[hep-ph\]](#)[Search inSPIRE](#)].
- [110] A. E. Cárcamo Hernández, L. T. Hue, S. Kovalenko, and H. N. Long, Eur. Phys. J. Plus **136**, 1158 (2021) [[arXiv:2001.01748 \[hep-ph\]](#)[Search inSPIRE](#)].
- [111] H. T. Hung, N. T. Tham, T. T. Hieu, and N. T. T. Hang, Prog. Theor. Exp. Phys. **2021**, 083B01 (2021) [[arXiv:2103.16018 \[hep-ph\]](#)[Search inSPIRE](#)].
- [112] J. C. Montero, F. Pisano, and V. Pleitez, Phys. Rev. D **47**, 2918 (1993) [[arXiv:hep-ph/9212271](#)[Search inSPIRE](#)].
- [113] M. Singer, J. W. F. Valle, and J. Schechter, Phys. Rev. D **22**, 738 (1980).
- [114] P. H. Frampton, Phys. Rev. Lett. **69**, 2889 (1992).
- [115] F. Pisano and V. Pleitez, Phys. Rev. D **46**, 410 (1992) [[arXiv:hep-ph/9206242](#)[Search inSPIRE](#)].
- [116] M. Lindner, M. Platscher, and F. S. Queiroz, Phys. Rept. **731**, 1 (2018) [[arXiv:1610.06587 \[hep-ph\]](#)[Search inSPIRE](#)].

- [117] A. S. De Jesus, S. Kovalenko, F. S. Queiroz, C. Siqueira, and K. Sinha, Phys. Rev. D **102**, 035004 (2020) [[arXiv:2004.01200 \[hep-ph\]](#)] [Search inSPIRE](#).
- [118] Á. S. de Jesus, S. Kovalenko, F. S. Queiroz, C. A. de S. Pires, and Y. S. Villamizar, Phys. Lett. B **809**, 135689 (2020) [[arXiv:2003.06440 \[hep-ph\]](#)] [Search inSPIRE](#).
- [119] A. E. C. Hernández, D. T. Huong, and I. Schmidt, Eur. Phys. J. C **82**, 63 (2022) [[arXiv:2109.12118 \[hep-ph\]](#)] [Search inSPIRE](#).
- [120] L. T. Hue, K. H. Phan, T. P. Nguyen, H. N. Long, and H. T. Hung, Eur. Phys. J. C **82**, 722 (2022) [[arXiv:2109.06089 \[hep-ph\]](#)] [Search inSPIRE](#).
- [121] S. M. Boucenna, J. W. F. Valle, and A. Vicente, Phys. Rev. D **92**, 053001 (2015) [[arXiv:1502.07546 \[hep-ph\]](#)] [Search inSPIRE](#).
- [122] D. Chang and H. N. Long, Phys. Rev. D **73**, 053006 (2006) [[arXiv:hep-ph/0603098](#)] [Search inSPIRE](#).
- [123] A. J. Buras, F. De Fazio, J. Girkbach, and M. V. Carlucci, J. High Energy Phys. **02**, 023 (2013) [[arXiv:1211.1237 \[hep-ph\]](#)] [Search inSPIRE](#).
- [124] H. K. Dreiner, H. E. Haber, and S. P. Martin, Phys. Rept. **494**, 1 (2010) [[arXiv:0812.1594 \[hep-ph\]](#)] [Search inSPIRE](#).
- [125] L. Ninh and H. N. Long, Phys. Rev. D **72**, 075004 (2005) [[arXiv:hep-ph/0507069](#)] [Search inSPIRE](#).
- [126] L. T. Hue, L. D. Ninh, T. T. Thuc, and N. T. T. Dat, Eur. Phys. J. C **78**, 128 (2018) [[arXiv:1708.09723 \[hep-ph\]](#)] [Search inSPIRE](#).
- [127] H. Okada, N. Okada, Y. Orikasa, and K. Yagyu, Phys. Rev. D **94**, 015002 (2016) [[arXiv:1604.01948 \[hep-ph\]](#)] [Search inSPIRE](#).
- [128] H. T. Hung, T. T. Hong, H. H. Phuong, H. L. T. Mai, and L. T. Hue, Phys. Rev. D **100**, 075014 (2019) [[arXiv:1907.06735 \[hep-ph\]](#)] [Search inSPIRE](#).
- [129] A. Crivellin, M. Hoferichter, and P. Schmidt-Wellenburg, Phys. Rev. D **98**, 113002 (2018) [[arXiv:1807.11484 \[hep-ph\]](#)] [Search inSPIRE](#).
- [130] F. Jegerlehner and A. Nyffeler, Phys. Rept. **477**, 1 (2009) [[arXiv:0902.3360 \[hep-ph\]](#)] [Search inSPIRE](#).
- [131] A. Denner, S. Heinemeyer, I. Puljak, D. Rebuzzi, and M. Spira, Eur. Phys. J. C **71**, 1753 (2011) [[arXiv:1107.5909 \[hep-ph\]](#)] [Search inSPIRE](#).
- [132] P. A. Zyla[Particle Data Group] et al. [Particle Data Group], Prog. Theor. Exp. Phys. **2020**, 083C01 (2020).
- [133] K. Abe[T2K Collaboration] et al. [T2K Collaboration], Nature **580**, 339 (2020); **583**, E16 (2020) [erratum] [[arXiv:1910.03887 \[hep-ex\]](#)] [Search inSPIRE](#).
- [134] M. Tanabashi[Particle Data Group] et al. [Particle Data Group], Phys. Rev. D **98**, 030001 (2018).
- [135] G. 't Hooft and M. J. G. Veltman, Nucl. Phys. B **44**, 189 (1972).
- [136] A. Denner and S. Dittmaier, Nucl. Phys. B **734**, 62 (2006) [[arXiv:hep-ph/0509141](#)] [Search inSPIRE](#).
- [137] T. Hahn and M. Perez-Victoria, Comput. Phys. Commun. **118**, 153 (1999) [[arXiv:hep-ph/9807565](#)] [Search inSPIRE](#).
- [138] K. H. Phan, H. T. Hung, and L. T. Hue, Prog. Theor. Exp. Phys. **2016**, 113B03 (2016) [[arXiv:1605.07164 \[hep-ph\]](#)] [Search inSPIRE](#).
- [139] K. Enomoto, S. Kanemura, K. Sakurai, and H. Sugiyama, Phys. Rev. D **100**, 015044 (2019) [[arXiv:1904.07039 \[hep-ph\]](#)] [Search inSPIRE](#).
- [140] H. B. Camara, R. G. Felipe, and F. R. Joaquim, J. High Energy Phys. **05**, 021 (2021) [[arXiv:2012.04557 \[hep-ph\]](#)] [Search inSPIRE](#).
- [141] M. Nebot, J. F. Oliver, D. Palao, and A. Santamaria, Phys. Rev. D **77**, 093013 (2008) [[arXiv:0711.0483 \[hep-ph\]](#)] [Search inSPIRE](#).
- [142] E. Fernandez-Martinez, J. Hernandez-Garcia, and J. Lopez-Pavon, J. High Energy Phys. **08**, 033 (2016) [[arXiv:1605.08774 \[hep-ph\]](#)] [Search inSPIRE](#).
- [143] N. R. Agostinho, G. C. Branco, P. M. F. Pereira, M. N. Rebelo, and J. I. Silva-Marcos, Eur. Phys. J. C **78**, 895 (2018) [[arXiv:1711.06229 \[hep-ph\]](#)] [Search inSPIRE](#).
- [144] A. M. Coutinho, A. Crivellin, and C. A. Manzari, Phys. Rev. Lett. **125**, 071802 (2020) [[arXiv:1912.08823 \[hep-ph\]](#)] [Search inSPIRE](#).
- [145] C. A. Manzari, A. M. Coutinho, and A. Crivellin, PoS **LHCP2020**, 242 (2021) [[arXiv:2009.03877 \[hep-ph\]](#)] [Search inSPIRE](#).